High order ADER schemes for a unified first order SHTC formulation of Newtonian and general relativistic continuum mechanics

Michael Dumbser

H2020 FET-HPC Grant *ExaHyPE,* nr. 671698

ERC Grant *STiMulUs,* nr. 278267

ECT* Workshop, 10/05/2018, Trento, Italy

European Research Council

Very General Form of the Governing PDE

We want to construct numerical schemes for **very general** hyperbolic-parabolic **systems** of **nonlinear** time-dependent partial differential equations in multiple space dimensions of the following general form:

$$\frac{\partial Q}{\partial t} + \nabla \cdot F(Q, \nabla Q) + B(Q) \cdot \nabla Q = S(Q) \qquad \text{(PDE)}$$

The nonlinear flux tensor **F** can also depend on the gradient of *Q,* to take into account **parabolic terms**, such as **classical** models for **viscous effects**. The third term is a **non-conservative** term that is important in many multi-phase flow models, and also for first order reductions of the **3+1 Einstein field equations**!
The source term on the right hand side may also be **stiff**.

Many of the mathematical models relevant for science and engineering can be cast in the form of eqn. (PDE).

Main difficulty: solutions of (PDE) can contain smooth features and discontinuities at the same time.

Unlimited Fully Discrete One-Step ADER-DG Scheme

Governing hyperbolic PDE system of the form

$$\frac{\partial \mathbf{Q}}{\partial t} + \nabla \cdot \mathbf{F}(\mathbf{Q}) = 0 \qquad \text{(PDE)}$$

with the vector of conserved variables **Q** and the nonlinear flux tensor **F**(**Q**). The discrete solution at time t^n is represented by piecewise polynomials of degree N over spatial control volumes T_i as

$$\mathbf{u}_h\left(\mathbf{x}, t^n\right) = \sum_l \Phi_l(\mathbf{x})\hat{\mathbf{u}}_l^n, \quad \mathbf{x} \in T_i \qquad \text{(DG)}$$

Multiplication with a test function ϕ_k from the space of piecewise polynomias of degree N and integration over a space-time control volume T_i x $[t^n, t^{n+1}]$ yields:

$$\int_{t^n}^{t^{n+1}} \int_{T_i} \Phi_k \frac{\partial \mathbf{Q}}{\partial t} d\mathbf{x}dt + \int_{t^n}^{t^{n+1}} \int_{\partial T_i} \Phi_k \mathbf{F}(\mathbf{Q}) \cdot \mathbf{n}\, dS dt - \int_{t^n}^{t^{n+1}} \int_{T_i} \nabla \Phi_k \cdot \mathbf{F}(\mathbf{Q}) d\mathbf{x}dt = 0$$

Unlimited Fully Discrete One-Step ADER-DG Scheme

We then introduce the discrete solution (DG) and an **element-local space-time predictor $\mathbf{q}_h(\mathbf{x},t)$,** together with a classical (monotone) numerical flux *G,* as it is used in Godunov-type finite volume schemes.

The fully discrete one-step ADER-DG scheme then simply reads:

$$\left(\int_{T_i} \Phi_k \Phi_l d\mathbf{x} \right) \left(\hat{\mathbf{u}}_l^{n+1} - \hat{\mathbf{u}}_l^n \right) + \int_{t^n}^{t^{n+1}} \int_{\partial T_i} \Phi_k \mathcal{G}\left(\mathbf{q}_h^-, \mathbf{q}_h^+ \right) \cdot \mathbf{n} \, dS dt - \int_{t^n}^{t^{n+1}} \int_{T_i} \nabla \Phi_k \cdot \mathbf{F}(\mathbf{q}_h) d\mathbf{x} dt = 0$$

But how to compute the space-time predictor $\mathbf{q}_h(\mathbf{x},t)$, since at the beginning of a time step, only the discrete spatial solution $\mathbf{u}_h(\mathbf{x},t^n)$ at time t^n is known?

Use a weak integral form of the PDE in space-time and solve an element-local Cauchy problem *in the small,* with initial data $\mathbf{u}_h(\mathbf{x},t^n)$, similar to the MUSCL-Hancock scheme or the ENO scheme of Harten et al.

Element-local Space-time Predictor

Rewrite the governing PDE in a reference coordinate system ξ-τ on a reference element T_E:

$$\frac{\partial \mathbf{Q}}{\partial \tau} + \nabla_\xi \cdot \mathbf{F}^*(\mathbf{Q}) = 0, \qquad \mathbf{F}^* := \Delta t (\partial \boldsymbol{\xi} / \partial \mathbf{x})^T \cdot \mathbf{F}(\mathbf{Q}).$$

We introduce the two space-time integral operators

$$\langle f, g \rangle = \int_0^1 \int_{T_E} (f(\boldsymbol{\xi}, \tau) \cdot g(\boldsymbol{\xi}, \tau)) d\boldsymbol{\xi}\, d\tau, \quad [f, g]^\tau = \int_{T_E} \big(f(\boldsymbol{\xi}, \tau) \cdot g(\boldsymbol{\xi}, \tau)\big) d\boldsymbol{\xi}$$

The discrete space-time predictor solution and the discrete flux are defined as

$$\mathbf{q}_h = \mathbf{q}_h(\boldsymbol{\xi}, \tau) = \sum_l \theta_l(\boldsymbol{\xi}, \tau) \hat{\mathbf{q}}_l := \theta_l \hat{\mathbf{q}}_l,$$

nodal space-time basis θ_l

$$\mathbf{F}_h^* = \mathbf{F}_h^*(\boldsymbol{\xi}, \tau) = \sum_l \theta_l(\boldsymbol{\xi}, \tau) \hat{\mathbf{F}}_l^* := \theta_l \hat{\mathbf{F}}_l^*, \qquad \hat{\mathbf{F}}_l^* = \mathbf{F}^*(\hat{\mathbf{q}}_l).$$

Element-local Space-time Predictor

Multiplication with a **space-time** test function and integration over the space-time reference element T_E x [0,1] yields:

$$\left\langle \theta_k, \frac{\partial \mathbf{q}_h}{\partial \tau} \right\rangle + \langle \theta_k, \nabla_\xi \cdot \mathbf{F}_h^*(\mathbf{q}_h) \rangle = 0.$$

The initial condition $\mathbf{u}_h(\mathbf{x},t^n)$ is introduced in a **weak sense** after integration by parts **in time** (upwinding in time, causality principle)**:**

$$[\theta_k, \mathbf{q}_h]^1 - [\theta_k, \mathbf{u}_h]^0 - \left\langle \frac{\partial}{\partial \tau}\theta_k, \mathbf{q}_h \right\rangle + \langle \theta_k, \nabla_\xi \cdot \mathbf{F}_h^* \rangle = 0.$$

The above element-local nonlinear system is easily solved via the following fast-converging fixed-point iteration (discrete Picard iteration):

$$\left([\theta_k, \theta_l]^1 - \left\langle \frac{\partial}{\partial \tau}\theta_k, \theta_l \right\rangle \right) \hat{\mathbf{q}}_l^{r+1} = [\theta_k, \Phi_l]^0 \hat{\mathbf{u}}_l^n - \langle \theta_k, \nabla_\xi \theta_l \rangle \cdot \mathbf{F}^*(\hat{\mathbf{q}}_l^r),$$

A new *a posteriori* limiter of DG-FEM methods

- Conventional DG limiters use either artificial viscosity, which needs parameters to be tuned, or nonlinear FV-type reconstruction/limiters (TVB, WENO, HWENO), which **usually destroy** the subcell resolution properties.
- Our new approach extends the successful *a posteriori* **MOOD** method of Loubère et al., developed in the FV context, also to the DG-FEM framework.
- As **very simple** *a posteriori* detection criteria, we only use
  - A relaxed discrete maximum principle (**DMP**) in the sense of polynomials
  - **Positivity** of the solution and absence of floating point errors (**NaN**)
- If one of these criteria is violated after a time step, the scheme **goes back** to the old time step and **recomputes** the solution in the troubled cells, using a more robust ADER-WENO or TVD FV scheme **on a <u>fine subgrid</u>** composed of ***2N+1*** subcells per space dimension

A new *a posteriori* limiter of DG-FEM methods

- Classical DG limiters, like WENO/HWENO/slope/moment limiters are based on **nonlinear data post-processing**, while the new DG limiter **recomputes** the discrete solution with a more robust scheme, starting again from a **valid solution** available at the old time level (the limiter is based on the PDE!!)
- Alternative description: dynamic, element-local **checkpointing** and **restarting** of the solver with a more robust scheme on a finer grid
- This enables the limiter even to **cure** floating point errors (**NaN** values appearing after division by zero or after taking roots of negative numbers)
- The new method is by construction **positivity preserving**, **iff** the underlying finite volume scheme on the subgrid preserves positivity
- **Local limiter** (in contrast to WENO limiters for DG), since it requires only information from the cell and its direct neighborhood
- As **accurate** as a high order **unlimited DG scheme** in smooth flow regions, but at the same time as **robust** as a **second order TVD scheme** at shocks or other discontinuities, but also at strong rarefactions

Classical TVB slope/moment limiting of DG

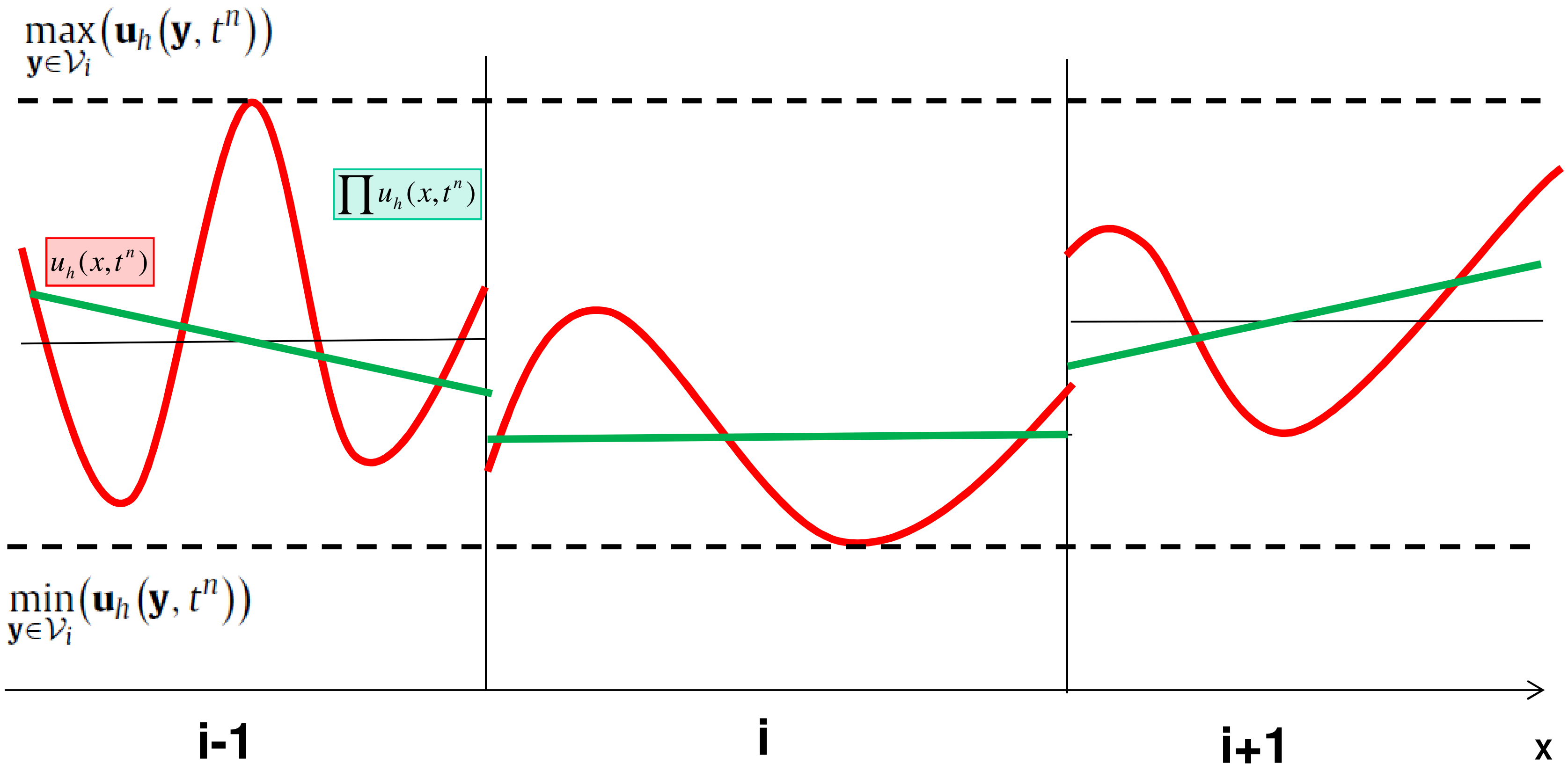

If a classical nonlinear reconstruction-based DG limiter is activated erroneously, there may be important physical information that is lost forever!

A new *a posteriori* limiter of DG-FEM methods

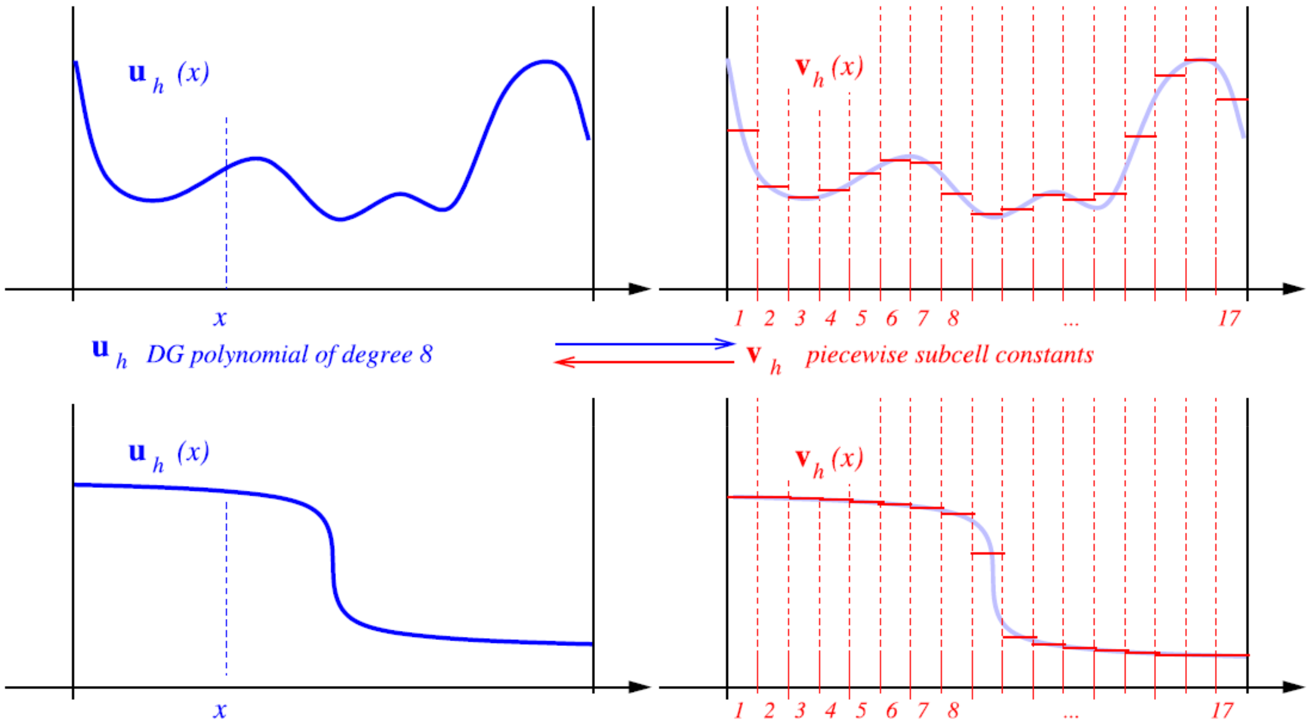

DG polynomials of degree *N*=8 (left) and **equivalent** data representation on *2N+1*=17 **subcells** (right). Arrows indicate projection (red) and reconstruction (blue)

$$\boxed{\mathcal{R} \circ \mathcal{P} = \mathcal{I}}$$

We use *2N+1* subcells to **match** the DG time step (CFL<*1/(2N+1)*) on the coarse grid with the FV time step (CFL<1) on the fine subgrid.

A new *a posteriori* limiter of DG-FEM methods

Projection from the DG polynomials to the subcell averages

$$\mathbf{v}_{i,j}^{n} = \frac{1}{|S_{i,j}|} \int_{S_{i,j}} \mathbf{u}_h(\mathbf{x}, t^n) d\mathbf{x} = \frac{1}{|S_{i,j}|} \int_{S_{i,j}} \phi_l(\mathbf{x}) d\mathbf{x}\, \hat{\mathbf{u}}_l^n, \quad \forall S_{i,j} \in \mathcal{S}_i.$$

Reconstruction of DG polynomials from the subcell averages

$$\int_{S_{i,j}} \mathbf{u}_h(\mathbf{x}, t^n) d\mathbf{x} = \int_{S_{i,j}} \mathbf{v}_h(\mathbf{x}, t^n) d\mathbf{x}, \quad \forall S_{i,j} \in \mathcal{S}_i.$$

$$\int_{T_i} \mathbf{u}_h(\mathbf{x}, t^n) d\mathbf{x} = \int_{T_i} \mathbf{v}_h(\mathbf{x}, t^n) d\mathbf{x}.$$

Linear constraint: conservation

Overdetermined system, solved by a constrained LSQ algorithm.

Summary of the ADER-DG-MOOD scheme

Verification of the DMP and the positivity on the **candidate solution $\mathbf{u}_h^*(\mathbf{x},t^{n+1})$:**

$$\min_{\mathbf{y}\in\mathcal{V}_i}\left(\mathbf{v}_h\left(\mathbf{y},t^n\right)\right)-\delta\leq\mathbf{v}_h^*\left(\mathbf{x},t^{n+1}\right)\leq\max_{\mathbf{y}\in\mathcal{V}_i}\left(\mathbf{v}_h\left(\mathbf{y},t^n\right)\right)+\delta,\quad\forall\mathbf{x}\in T_i,$$

$$\pi_k\left(\mathbf{u}_h^*\left(\mathbf{x},t^{n+1}\right)\right)>0,\quad\forall\mathbf{x}\in T_i,\ \forall k,$$

If a cell does not satisfy both criteria, flag it as troubled cell, $\beta_i^{n+1}=1$, **discard** the DG solution and **recompute** it with a more robust third order **ADER-WENO** or an even more robust **second order TVD finite** volume scheme on the **fine subgrid**:

$$\mathbf{v}_h\left(\mathbf{x},t^{n+1}\right)=\mathcal{A}\left(\mathbf{v}_h\left(\mathbf{x},t^n\right)\right)$$

$$\mathbf{v}_h(\mathbf{x},t^n)=\begin{cases}\mathcal{P}\left(\mathbf{u}_h(\mathbf{x},t^n)\right) & \text{if}\quad \beta_j^n=0,\\ \mathcal{A}(\mathbf{v}_h(\mathbf{x},t^{n-1})) & \text{if}\quad \beta_j^n=1.\end{cases}\qquad \mathbf{x}\in T_j\qquad \forall T_j\in\mathcal{V}_i.$$

Finally, **reconstruct** the DG polynomial from the subcell averages:

$$\mathbf{u}_h\left(\mathbf{x},t^{n+1}\right)=\mathcal{R}\left(\mathbf{v}_h\left(\mathbf{x},t^{n+1}\right)\right)\qquad\text{or}\qquad\boxed{\mathbf{u}_h\left(\mathbf{x},t^{n+1}\right)=\mathcal{R}\left(\mathcal{A}\left(\mathbf{v}_h\left(\mathbf{x},t^n\right)\right)\right)}$$

Numerical Convergence Results P2-P9 (2D Euler)

	N_x	L^1 error	L^2 error	L^∞ error	L^1 order	L^2 order	L^∞ order	Theor.
DG-$\mathbb{P}_2$	25	9.33E−03	2.07E−03	2.02E−03	–	–	–	3
	50	6.70E−04	1.58E−04	1.66E−04	3.80	3.71	3.60	
	75	1.67E−04	4.07E−05	4.45E−05	3.43	3.35	3.25	
	100	6.74E−05	1.64E−05	1.82E−05	3.15	3.15	3.10	
DG-$\mathbb{P}_3$	25	5.77E−04	9.42E−05	7.84E−05	–	–	–	4
	50	2.75E−05	4.52E−06	4.09E−06	4.39	4.38	4.26	
	75	4.36E−06	7.89E−07	7.55E−07	4.55	4.30	4.17	
	100	1.21E−06	2.37E−07	2.38E−07	4.46	4.17	4.01	
DG-$\mathbb{P}_4$	20	1.54E−04	2.18E−05	2.20E−05	–	–	–	5
	30	1.79E−05	2.46E−06	2.13E−06	5.32	5.37	5.75	
	40	3.79E−06	5.35E−07	5.18E−07	5.39	5.31	4.92	
	50	1.11E−06	1.61E−07	1.46E−07	5.50	5.39	5.69	
DG-$\mathbb{P}_5$	10	9.72E−04	1.59E−04	2.00E−04	–	–	–	6
	20	1.56E−05	2.13E−06	2.14E−06	5.96	6.22	6.55	
	30	1.14E−06	1.64E−07	1.91E−07	6.45	6.33	5.96	
	40	2.17E−07	2.97E−08	3.59E−08	5.77	5.93	5.82	
DG-$\mathbb{P}_6$	5	2.24E−02	4.15E−03	3.11E−03	–	–	–	7
	10	1.76E−04	2.75E−05	2.86E−05	6.99	7.24	6.76	
	20	1.67E−06	2.28E−07	2.26E−07	6.72	6.91	6.98	
	25	3.60E−07	4.96E−08	6.27E−08	6.86	6.84	5.74	
DG-$\mathbb{P}_7$	5	5.50E−03	1.22E−03	1.46E−03	–	–	–	8
	10	4.63E−05	6.26E−06	6.95E−06	6.89	7.61	7.71	
	15	1.62E−06	2.20E−07	2.29E−07	8.28	8.26	8.42	
	20	2.05E−07	2.80E−08	2.28E−08	7.18	7.17	8.01	
DG-$\mathbb{P}_8$	4	9.11E−03	1.80E−03	3.44E−03	–	–	–	9
	8	4.97E−05	7.51E−06	6.93E−06	7.52	7.90	8.96	
	10	7.50E−06	1.05E−06	1.18E−06	8.47	8.81	7.95	
	15	2.40E−07	3.34E−08	3.09E−08	8.49	8.51	8.98	
DG-$\mathbb{P}_9$	4	3.95E−03	7.89E−04	1.42E−03	–	–	–	10
	8	1.01E−05	1.44E−06	1.52E−06	8.61	9.09	9.87	
	10	1.44E−06	2.00E−07	2.27E−07	8.74	8.85	8.51	
	12	2.67E−07	3.70E−08	3.77E−08	9.26	9.25	9.85	

ADER-DG-MOOD Results

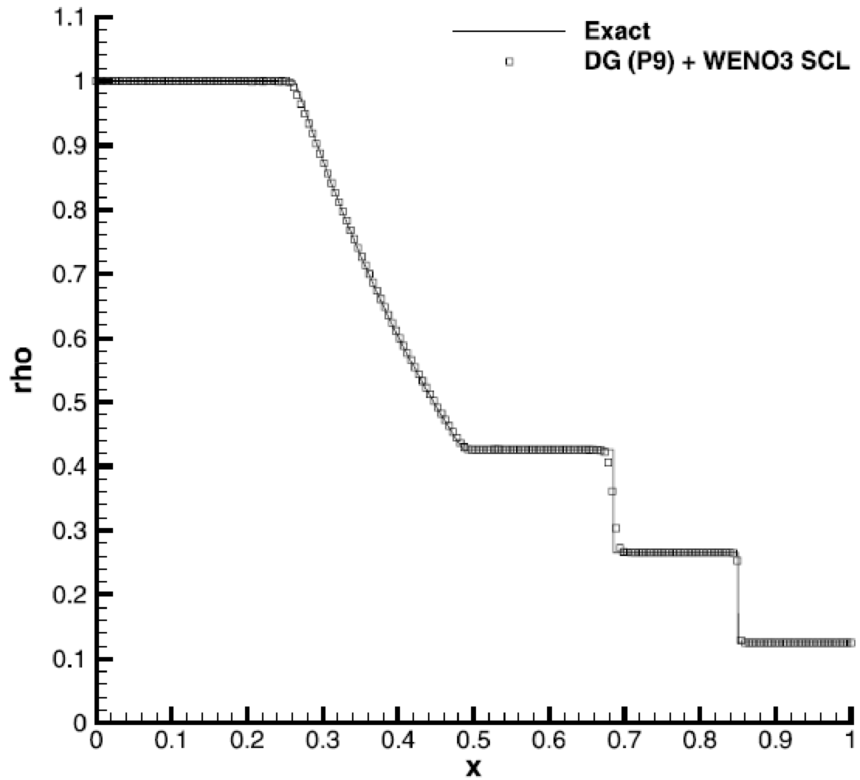

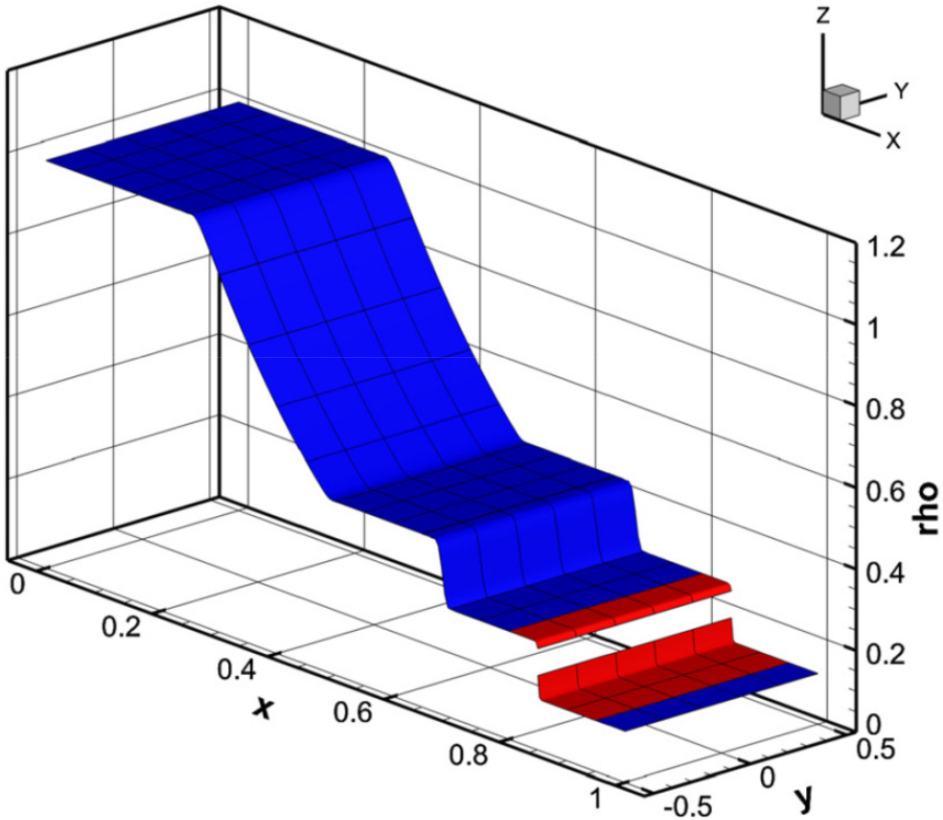

Sod shock tube,
20x5 elements (N=9)

Limited cells (red),
Unlimited cells (blue)

ADER-DG-MOOD Results

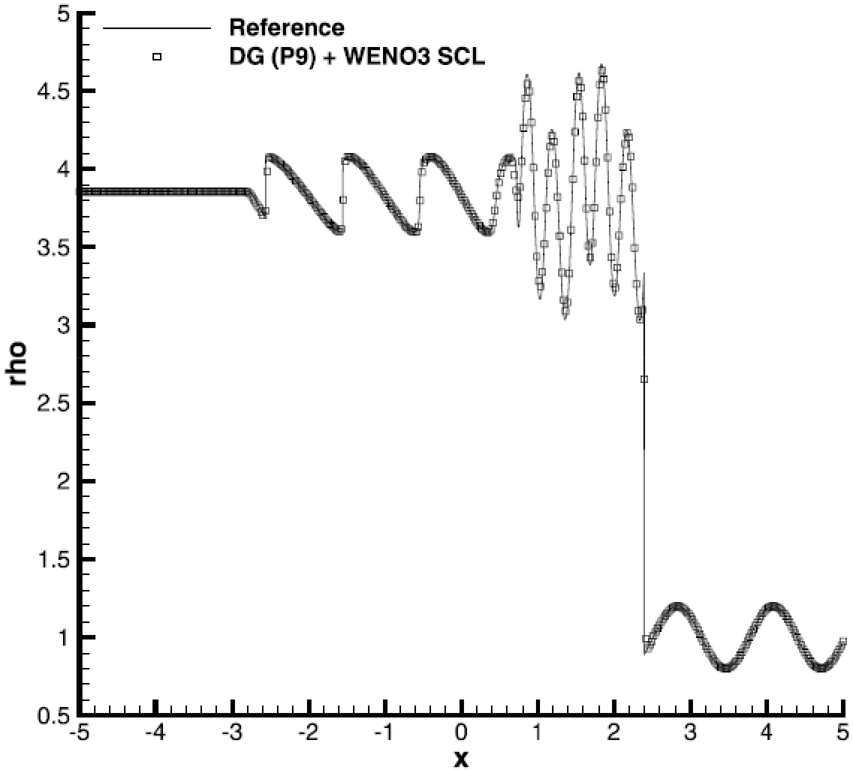

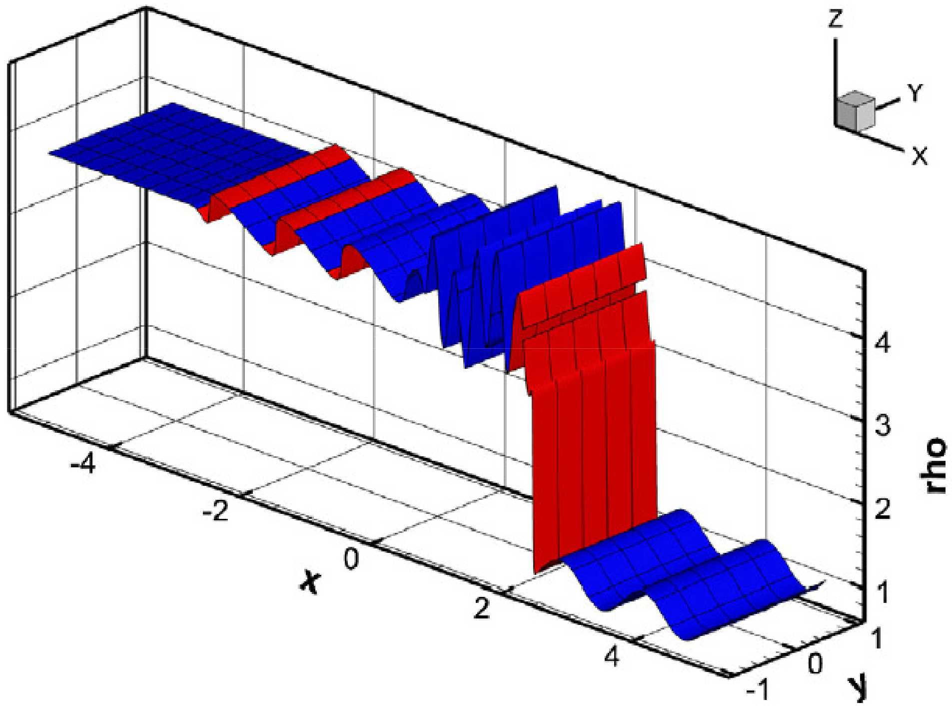

Shock-density interaction problem of Shu & Osher
40x5 cells (N=9). Unlimited cells (blue) and limited cells (red)

Extension to high order AMR: Grid and Data Structure

One refinement level & virtual cells

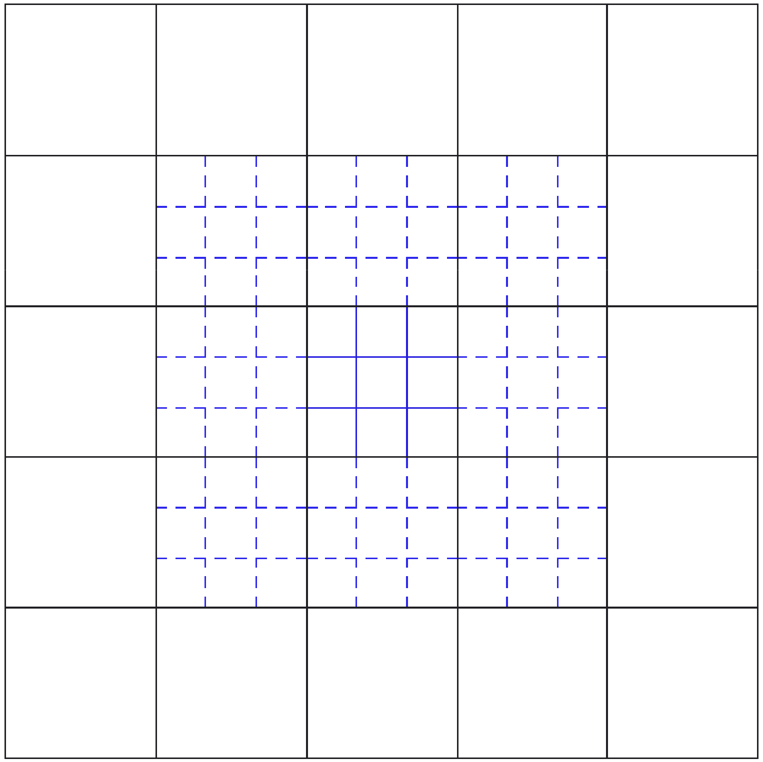

Two refinement levels & virtual cells

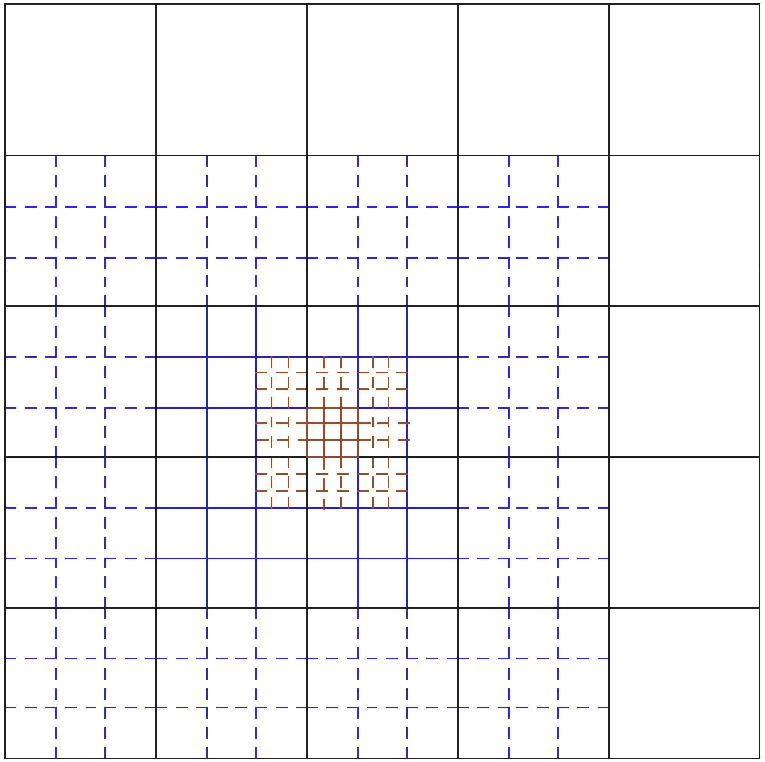

AMR with Time-Accurate Local Time Stepping (LTS)

Within our **ADER-DG** one-step predictor-corrector approach, high order **time-accurate** and fully *conservative* **local time stepping** (LTS) is **straightforward**:

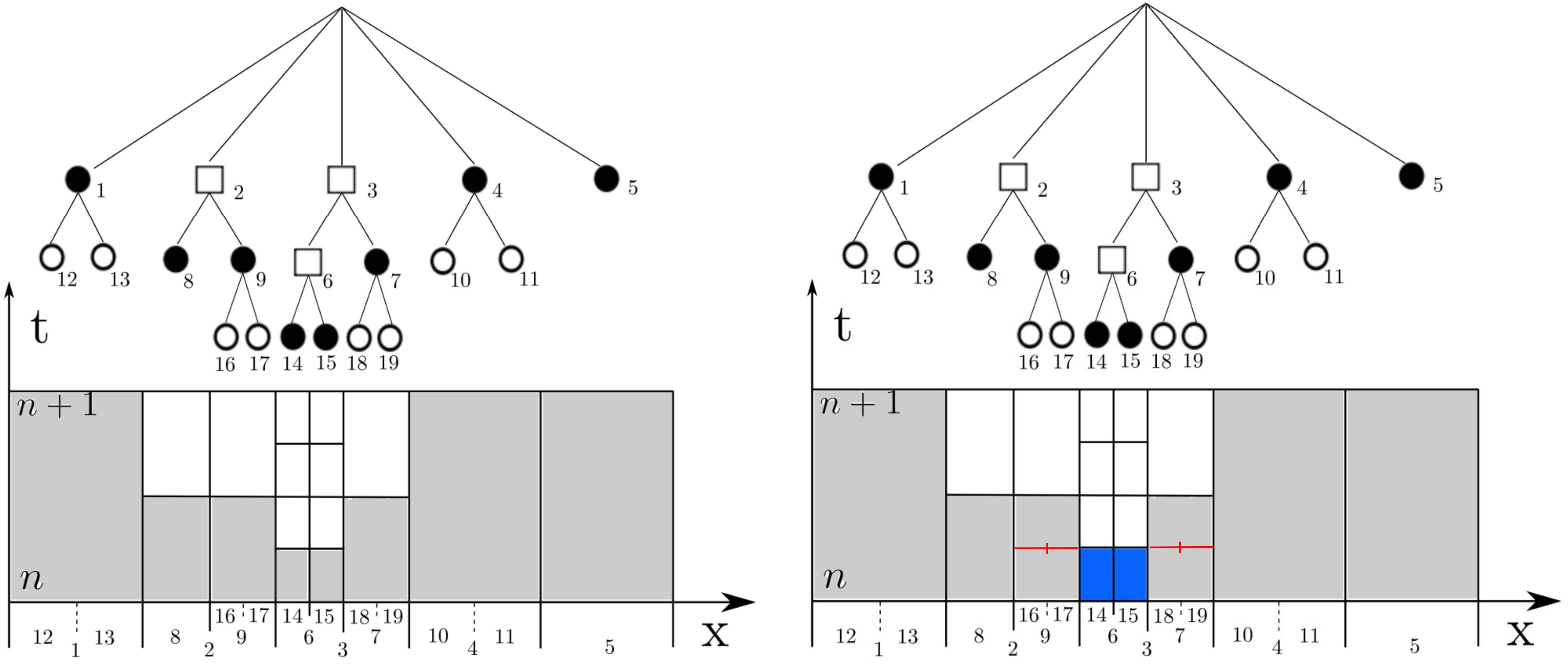

A posteriori subcell limiters with AMR (Euler equations)

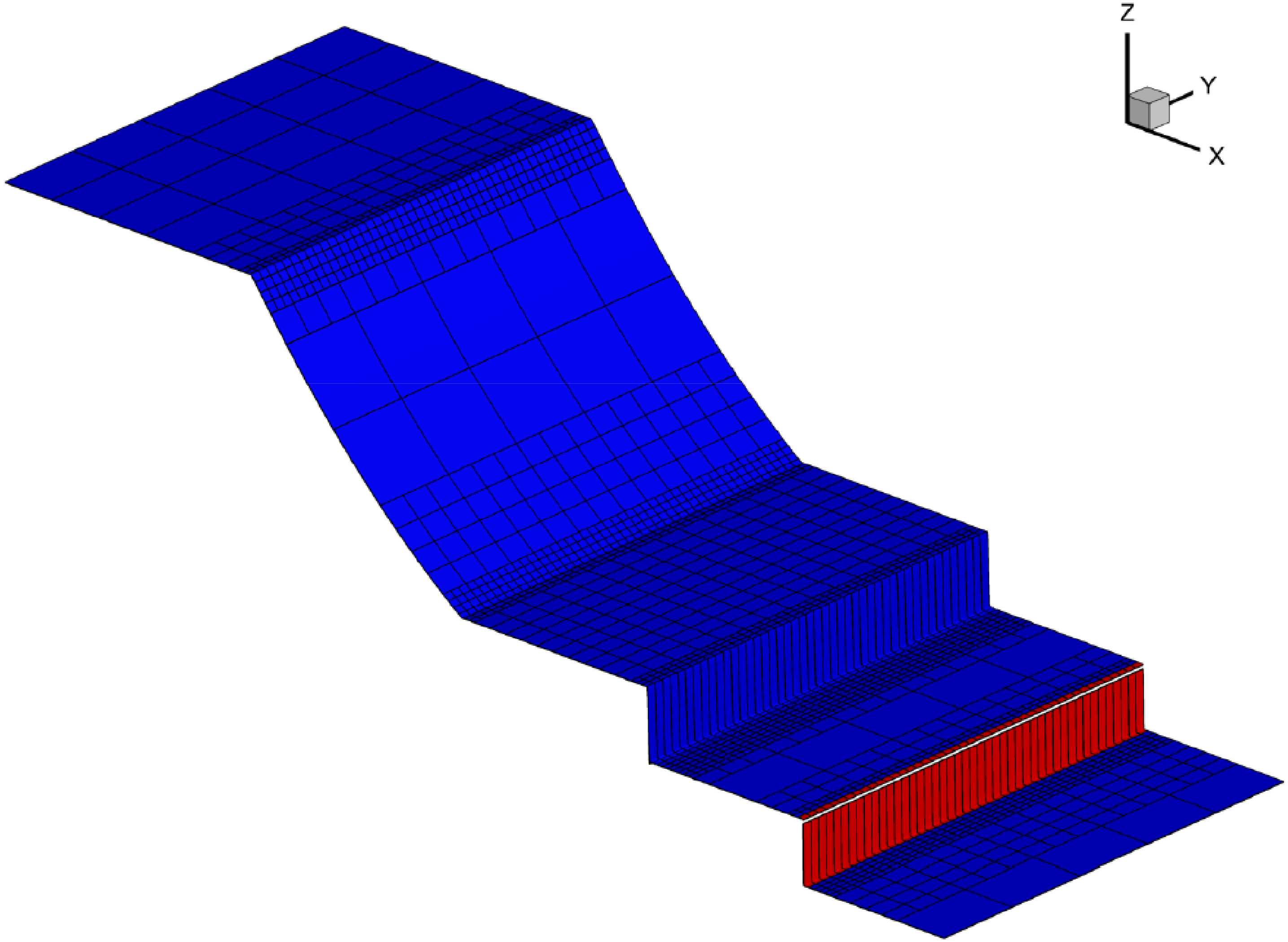

M. Dumbser

ADER-DG (N=9) with AMR & LTS. Unlimited cells (blue) and limited cells (red)

A posteriori subcell limiters with AMR (Euler equations)

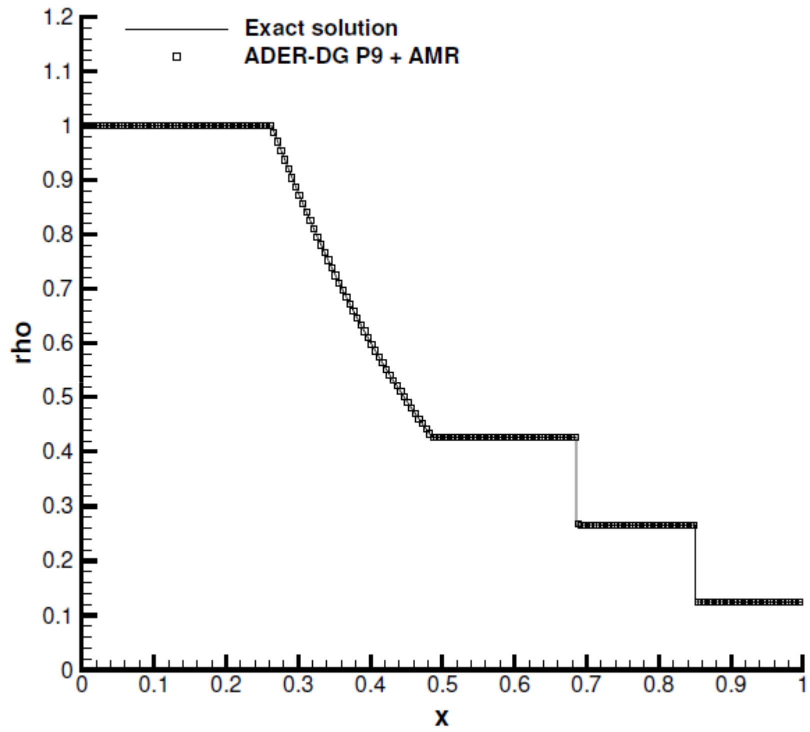

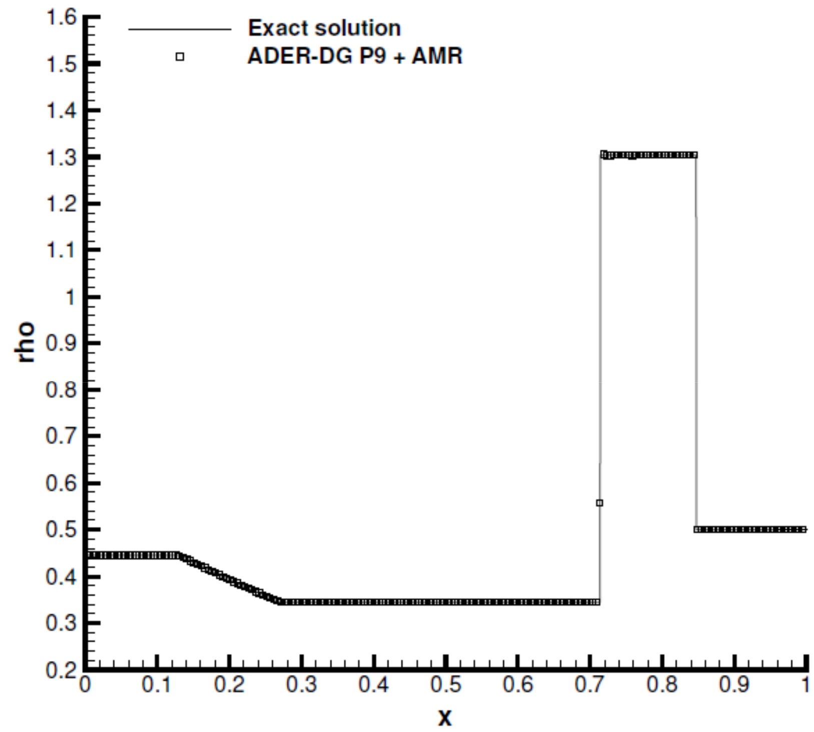

ADER-DG (N=9) with a posteriori ADER-WENO subcell limiter, space-time adaptive mesh refinement (AMR) and LTS yields an unprecedented resolution of shocks and contact waves.

A posteriori subcell limiters with AMR (Euler equations)

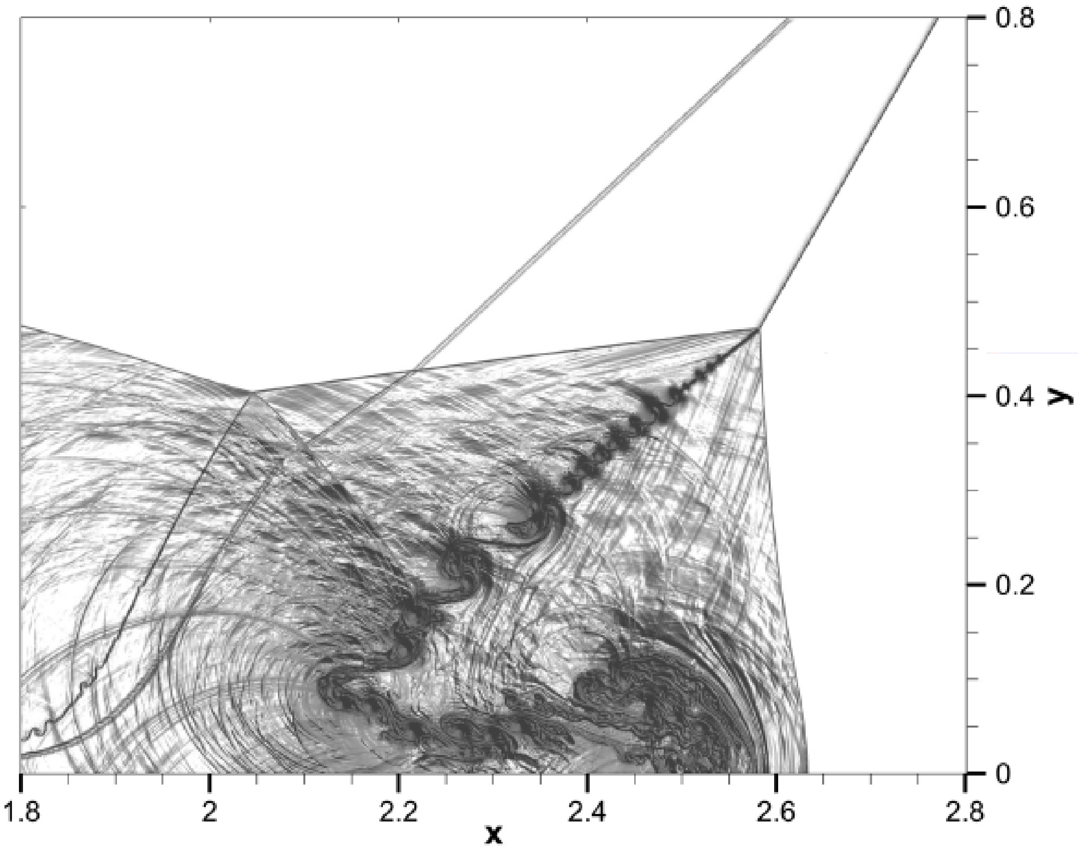

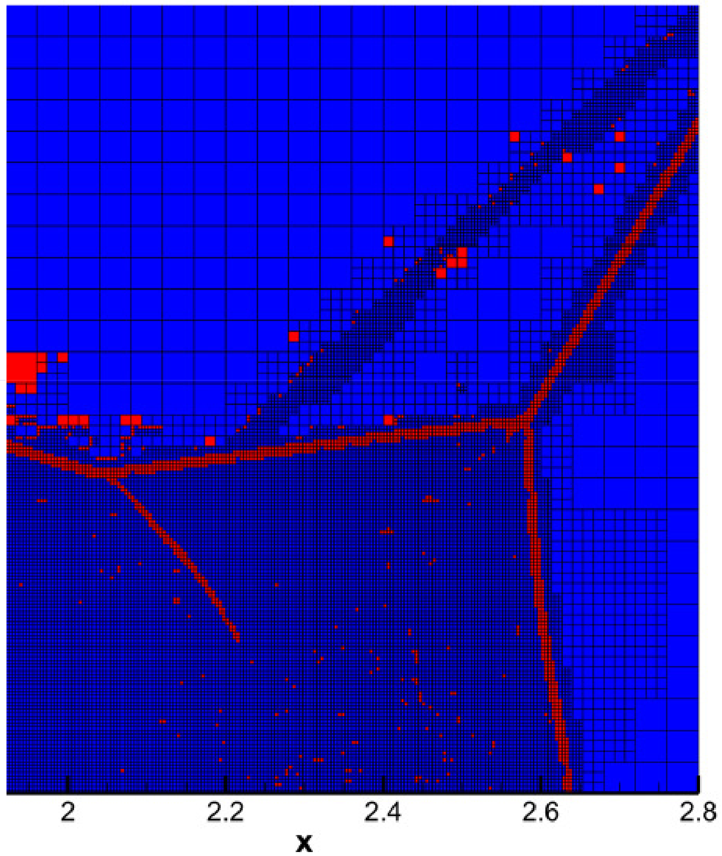

Double Mach reflection problem using ADER-DG (N=9) with a posteriori ADER-WENO subcell limiter, space-time adaptive mesh refinement (AMR) & LTS

First Order Hyperbolic Formulation of Continuum Mechanics

$$\frac{\partial \rho}{\partial t} + \frac{\partial \rho v_k}{\partial x_k} = 0, \quad \textbf{(1a)}$$

$$\frac{\partial \rho v_i}{\partial t} + \frac{\partial \left(\rho v_i v_k + p\delta_{ik} - \sigma_{ik}\right)}{\partial x_k} = 0, \quad \textbf{(1b)}$$

$$\frac{\partial A_{ik}}{\partial t} + \frac{\partial A_{im} v_m}{\partial x_k} + v_j \left(\frac{\partial A_{ik}}{\partial x_j} - \frac{\partial A_{ij}}{\partial x_k} \right) = -\frac{\psi_{ik}}{\theta_1(\tau_1)}, \quad \textbf{(1c)}$$

$$\frac{\partial \rho J_i}{\partial t} + \frac{\partial \left(\rho J_i v_k + T\delta_{ik}\right)}{\partial x_k} = -\frac{\rho H_i}{\theta_2(\tau_2)}, \quad \textbf{(1d)}$$

$$\frac{\partial \rho s}{\partial t} + \frac{\partial \left(\rho s v_k + H_k\right)}{\partial x_k} = \frac{\rho}{\theta_1(\tau_1) T}\psi_{ik}\psi_{ik} + \frac{\rho}{\theta_2(\tau_2) T} H_i H_i \geq 0, \quad \textbf{(1e)}$$

$$\frac{\partial \rho E}{\partial t} + \frac{\partial \left(v_k \rho E + v_i (p\delta_{ik} - \sigma_{ik}) + q_k\right)}{\partial x_k} = 0 \quad \textbf{(2)}$$

[Godunov & Romenski 1972, Peshkov & Romenski 2016] – GPR model

First Order Hyperbolic Formulation of Continuum Mechanics

Overdetermined PDE system, which is consistent if and only if the total energy *E* is a **potential** that depends on the other state variables:

$$E = E(\rho, s, \mathbf{v}, \mathbf{A}, \mathbf{J})$$

All the other fluxes (pressure, viscous stress tensor) and the dissipative source term are then a direct **consequence** of the choice of *E*:

Pressure: $p = \rho^2 E_\rho$

Temperature: $T = E_s$

Stress tensor: $[\sigma_{ik}] = \boldsymbol{\sigma} = -[\rho A_{mi} E_{A_{mk}}]$

Heat flux vector: $[q_k] = \mathbf{q} = [E_s E_{J_k}]$

Strain relaxation: $[\psi_{ik}] = \boldsymbol{\psi} = [E_{A_{ik}}]$ $\qquad \boldsymbol{\sigma} = -\rho \mathbf{A}^T \boldsymbol{\psi}$

Heat flux relaxation: $[H_i] = \mathbf{H} = [E_{J_i}]$ $\qquad \mathbf{q} = T\,\mathbf{H}$

Furthermore, some positive functions of the relaxation times τ_1 and τ_2:

$$\theta_1 = \theta_1(\tau_1) > 0 \qquad \theta_2 = \theta_2(\tau_2) > 0$$

First Order Hyperbolic Formulation of Continuum Mechanics

Choice of the total energy potential:

$$E(\rho, s, \mathbf{v}, \mathbf{A}, \mathbf{J}) = E_1(\rho, s) + E_2(\mathbf{A}, \mathbf{J}) + E_3(\mathbf{v}).$$

Classical equation of state, e.g. ideal gas EOS (micro-scale):

$$E_1(\rho, s) = \frac{c_0^2}{\gamma(\gamma - 1)}, \quad c_0^2 = \gamma \rho^{\gamma-1} e^{s/c_V}$$

adiabatic sound speed

Classical kinetic energy (macro-scale):

$$E_3(\mathbf{v}) = \frac{1}{2} v_i v_i$$

Energy stored in the <u>meso-scale</u>, due to <u>deformations</u> and <u>heat-flux</u>:

$$E_2(\mathbf{A}, \mathbf{J}) = \frac{c_s^2}{4} G_{ij}^{\mathrm{TF}} G_{ij}^{\mathrm{TF}} + \frac{\alpha^2}{2} J_i J_i$$

+ shear wave speed
+ heat wave speed

$$[G_{ij}^{\mathrm{TF}}] = \mathrm{dev}(\mathbf{G}) = \mathbf{G} - \frac{1}{3}\mathrm{tr}(\mathbf{G})\mathbf{I}, \qquad \text{and} \qquad \mathbf{G} = \mathbf{A}^{\mathsf{T}} \mathbf{A}.$$

First Order Hyperbolic Formulation of Continuum Mechanics

Stress tensor:

$$\boldsymbol{\sigma} = -\rho \mathbf{A}^{\mathsf{T}} \boldsymbol{\psi} = -\rho \mathbf{A}^{\mathsf{T}} E_A = -\rho c_s^2 \mathbf{G} \operatorname{dev}(\mathbf{G}) \qquad E_A = c_s^2 \mathbf{A} \operatorname{dev}(\mathbf{G})$$

Strain relaxation source term:

$$-\frac{\psi}{\theta_1(\tau_1)} = -\frac{E_A}{\theta_1(\tau_1)} = -\frac{3}{\tau_1} |\mathbf{A}|^{\frac{5}{3}} \mathbf{A} \operatorname{dev}(\mathbf{G})$$

with

$$\theta_1(\tau_1) = \tau_1 c_s^2 / 3 \, |\mathbf{A}|^{-\frac{5}{3}}$$

Heat flux vector:

$$\mathbf{q} = T\,\mathbf{H} = E_s E_{\mathbf{J}} = \alpha^2 T \mathbf{J} \qquad E_{\mathbf{J}} = \alpha^2 \mathbf{J}$$

Thermal impulse relaxation source term:

$$-\frac{\rho \mathbf{H}}{\theta_2(\tau_2)} = -\frac{\rho E_{\mathbf{J}}}{\theta_2(\tau_2)} = -\frac{T}{T_0} \frac{\rho_0}{\rho} \frac{\rho \mathbf{J}}{\tau_2}. \qquad \theta_2 = \tau_2 \alpha^2 \frac{\rho}{\rho_0} \frac{T_0}{T}$$

First Order Hyperbolic Formulation of Continuum Mechanics

Compatibility condition:

$$(E - VE_V - sE_s - v_i E_{v_i} - J_i E_{J_i}) \cdot (1\mathrm{a}) + (\rho E)_{\rho v_i} \cdot (1\mathrm{b}) +$$
$$+ (\rho E)_{A_{ik}} \cdot (1\mathrm{c}) + (\rho E)_{\rho J_i} \cdot (1\mathrm{d}) + (\rho E)_{\rho s} \cdot (1\mathrm{e}) \equiv (2)$$

The dissipative mechanisms on the right hand side of the GPR model are chosen such that total energy is conserved (first law of thermodynamics) and that entropy production is non-negative (second law of thermodynamics).

Use of the thermodynamic <u>dual</u> variables (factors above)

$$r = E - VE_V - sE_s - v_i E_{v_i} - J_i E_{J_i}, \quad v_i = (\rho E)_{\rho v_i},$$

$$\alpha_{ik} = (\rho E)_{A_{ik}}, \quad \Theta_i = (\rho E)_{\rho J_i}, \quad \sigma = (\rho E)_{\rho s}$$

and the Legendre transform of the potential *E* lead to the new potential

$$L(r, v_i, \alpha_{ik}, \Theta_i, \sigma) = r\rho + v_i \rho v_i + \alpha_{ik} A_{ik} + \Theta_i \rho J_i + \sigma \rho s - \rho E$$

First Order Hyperbolic Formulation of Continuum Mechanics

and to the following PDE system (only LHS shown here), which is also directly connected to a <u>variational formulation</u> (minimization of a Lagrangian):

$$\frac{\partial L_r}{\partial t} + \frac{\partial (v_k L)_r}{\partial x_k} = 0,$$

$$\frac{\partial L_{v_i}}{\partial t} + \frac{\partial (v_k L)_{v_i}}{\partial x_k} + L_{\alpha_{im}} \frac{\partial \alpha_{km}}{\partial x_k} - L_{\alpha_{mk}} \frac{\partial \alpha_{mk}}{\partial x_i} = 0,$$

$$\frac{\partial L_{\alpha_{il}}}{\partial t} + \frac{\partial (v_k L)_{\alpha_{il}}}{\partial x_k} + L_{\alpha_{ml}} \frac{\partial v_m}{\partial x_i} - L_{\alpha_{il}} \frac{\partial v_k}{\partial x_k} = 0,$$

$$\frac{\partial L_{\Theta_i}}{\partial t} + \frac{\partial (v_k L)_{\Theta_i}}{\partial x_k} + \frac{\partial \sigma \delta_{ik}}{\partial x_k} = 0,$$

$$\frac{\partial L_{\sigma}}{\partial t} + \frac{\partial (v_k L)_{\sigma}}{\partial x_k} + \frac{\partial \Theta_k}{\partial x_k} = 0,$$

The above system is <u>symmetric</u>. It is <u>hyperbolic</u>, iff the potential *L* is convex

$$\mathcal{M}(\mathbf{P}) \frac{\partial \mathbf{P}}{\partial t} + \mathcal{H}_k(\mathbf{P}) \frac{\partial \mathbf{P}}{\partial x_k} = 0 \qquad \mathcal{M}^{\mathsf{T}} = \mathcal{M} > 0 \quad \mathcal{H}_k^{\mathsf{T}} = \mathcal{H}_k$$

Hyperbolic formulation of Newtonian continuum physics

$$\frac{\partial \rho}{\partial t} + \frac{\partial \rho v_k}{\partial x_k} = 0,$$

$$\frac{\partial (\rho u_i)}{\partial t} + \frac{\partial (\rho u_i v_k + p\delta_{ik} - \sigma_{ik} + \beta_{ik})}{\partial x_k} = 0,$$

$$\frac{\partial A_{ik}}{\partial t} + \frac{\partial A_{im} v_m}{\partial x_k} + v_j \left(\frac{\partial A_{ik}}{\partial x_j} - \frac{\partial A_{ij}}{\partial x_k} \right) = -\frac{\psi_{ik}}{\theta_1(\tau_1)},$$

$$\frac{\partial (\rho J_i)}{\partial t} + \frac{\partial (\rho J_i v_k + T\delta_{ik})}{\partial x_k} = -\frac{\rho H_i}{\theta_2(\tau_2)},$$

$$\frac{\partial D_i}{\partial t} + \frac{\partial (v_k D_i - v_i D_k - \varepsilon_{ikl} b_l)}{\partial x_k} + v_i \frac{\partial D_k}{\partial x_k} = -\frac{1}{\eta} d_i,$$

$$\frac{\partial B_i}{\partial t} + \frac{\partial (v_k B_i - v_i B_k + \varepsilon_{ikl} d_l + \varphi \delta_{ik})}{\partial x_k} + v_i \frac{\partial B_k}{\partial x_k} = 0,$$

$$\frac{\partial (\rho E)}{\partial t} + \frac{\partial \left(v_k \rho E + v_i [p\delta_{ik} - \sigma_{ik} + \beta_{ik}] + \varepsilon_{ijk} d_i b_j + q_k \right)}{\partial x_k} = 0,$$

$$\frac{\partial (\rho s)}{\partial t} + \frac{\partial (\rho s v_k + H_k)}{\partial x_k} = \frac{\rho}{\theta_1(\tau_1) T} \psi_{ik} \psi_{ik} + \frac{\rho}{\theta_2(\tau_2) T} H_i H_i + \frac{1}{\eta T} d_i d_i \geq 0,$$

$$\boxed{\rho \mathbf{u} = \rho \mathbf{v} + \mu' \epsilon' \mathbf{d} \times \mathbf{b}}$$

Godunov (1961)
Godunov & Romenski (1972)
Romenski (1998)
Peshkov & Romenski (2016)
Dumbser et al. (2016)
Dumbser et al. (2017)

Hyperbolic formulation of Newtonian continuum physics

$$\frac{\partial L_r}{\partial t} + \frac{\partial[(v_k L)_r]}{\partial x_k} = 0,$$

$$\frac{\partial L_{v_i}}{\partial t} + \frac{\partial}{\partial x_k}\left[(v_k L)_{v_i} + \alpha_{mk} L_{\alpha_{mi}} - \delta_{ik}\alpha_{mn} L_{\alpha_{mn}} - d_i L_{d_k} - b_i L_{b_k}\right] = 0,$$

$$\frac{\partial L_{\alpha_{ik}}}{\partial t} + \frac{\partial[(v_m L)_{\alpha_{im}}]}{\partial x_k} + \varepsilon_{klj}\varepsilon_{lmn} v_j \frac{\partial L_{\alpha_{in}}}{\partial x_m} = -\frac{1}{\rho\theta_1}\alpha_{ik},$$

$$\frac{\partial L_{d_i}}{\partial t} + \frac{\partial[(v_k L)_{d_i} - v_i L_{d_k} - \varepsilon_{ikl} b_l]}{\partial x_k} + v_i \frac{\partial L_{d_k}}{\partial x_k} = -\frac{1}{\eta} d_i,$$

$$\frac{\partial L_{b_i}}{\partial t} + \frac{\partial[(v_k L)_{b_i} - v_i L_{b_k} + \varepsilon_{ikl} d_l]}{\partial x_k} + v_i \frac{\partial L_{b_k}}{\partial x_k} = 0,$$

$$\frac{\partial L_{\eta_i}}{\partial t} + \frac{\partial[(v_k L)_{\eta_i} + \delta_{ik} T]}{\partial x_k} = -\frac{\rho}{\theta_2}\eta_i,$$

$$\frac{\partial L_T}{\partial t} + \frac{\partial[(v_k L)_T + \eta_k]}{\partial x_k} = \frac{1}{\rho\theta_1}\alpha_{ik}\alpha_{ik} + \frac{1}{\eta} d_i d_i + \frac{\rho}{\theta_2}\eta_i\eta_i.$$

All dissipative terms have the **same** form as Ohm‘s law. PDE does **not** change type!

First Order Hyperbolic Formulation of Continuum Mechanics

Asymptotic (stiff) relaxation limit of the stress tensor:

$$\dot{\mathbf{G}} = \partial \mathbf{G}/\partial t + \mathbf{v} \cdot \nabla \mathbf{G} \qquad \mathbf{G} = \mathbf{A}^{\mathsf{T}}\mathbf{A}$$

$$\dot{\mathbf{G}} = -\left(\mathbf{G}\nabla\mathbf{v} + \nabla\mathbf{v}^{\mathsf{T}}\mathbf{G}\right) + \frac{2}{\rho\,\theta_1}\,\sigma.$$

Chapman-Enskog expansion of G...

$$\mathbf{G} = \mathbf{G}_0 + \tau_1 \mathbf{G}_1 + \tau_1^2 \mathbf{G}_2 + \ldots$$

... and after some tedious calculations ...

... in the stiff limit, the classical Navier-Stokes stress tensor is <u>recovered</u> as a <u>result</u> of the theory (it was never put *a priori* into the model)

$$\sigma = \frac{1}{6}\tau_1 \rho_0 c_s^2 \left(\nabla\mathbf{v} + \nabla\mathbf{v}^T - \frac{2}{3}\mathrm{tr}(\nabla\mathbf{v})\mathbf{I}\right) := \mu\left(\nabla\mathbf{v} + \nabla\mathbf{v}^T - \frac{2}{3}(\nabla\cdot\mathbf{v})\mathbf{I}\right),$$

First Order Hyperbolic Formulation of Continuum Mechanics

The relaxation time τ_1 and the shear wave speed c_s of the GPR model can be obtained **experimentally via ultra sound measurements** of the phase velocity of longitudinal pressure waves, which is **different** for low and high frequencies. This effect is well known in the research field of ultra-sound. It is **not predicted** by the classical Navier-Stokes equations of fluid mechanics, but by the GPR model!

$$\lambda_{5,6} = \pm\sqrt{c_0^2 + \tfrac{4}{3}c_s^2}$$

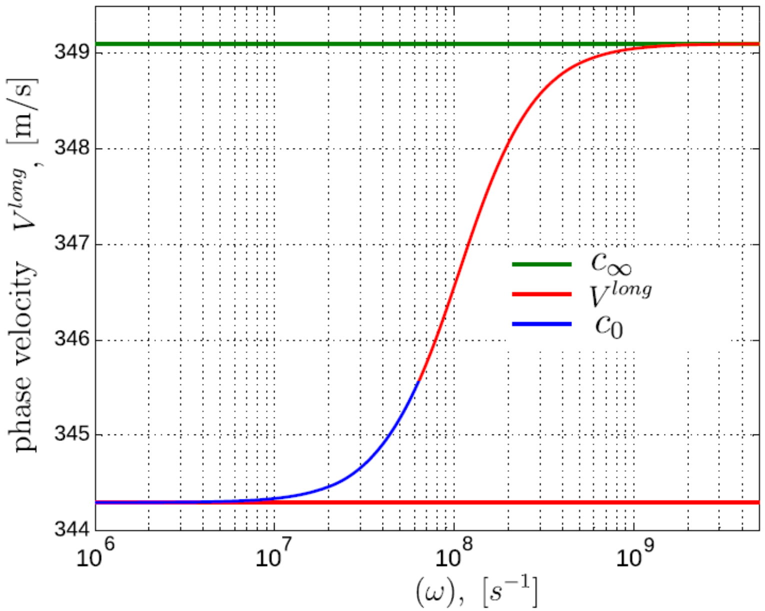

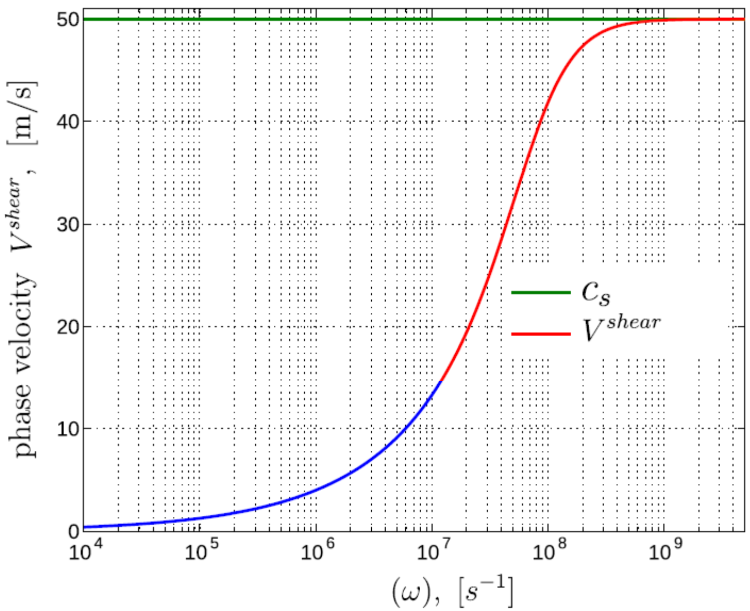

Fig. 1. Phase velocity of the longitudinal wave (left) and shear wave (right) versus $\log(\omega)$ propagating in a viscous gas with parameters $\rho = 1.177$ kg/m^3, $\gamma = 1.4$, $c_v = 718$ J/(kg K), $s = 8100$, $c_0 = 344.3$ m/s, $c_s = 50$ m/s, $\mu = 1.846 \cdot 10^{-5}$ Pa s, $\tau_1 = 3.76 \cdot 10^{-8}$ s.

Convergence rates for inviscid flow (GPR, stiff limit)

N_x	$\epsilon(L_1)$	$\epsilon(L_2)$	$\epsilon(L_\infty)$	$\mathcal{O}(L_1)$	$\mathcal{O}(L_2)$	$\mathcal{O}(L_\infty)$
			ADER-DG P_2P_2 ($\mu = \kappa = 10^{-6}$)			
20	9.4367E-03	2.2020E-03	2.1633E-03			
40	1.9524E-03	4.4971E-04	4.2688E-04	2.27	2.29	2.34
60	7.5180E-04	1.7366E-04	1.4796E-04	2.35	2.35	2.61
80	3.7171E-04	8.6643E-05	7.3988E-05	2.45	2.42	2.41
			ADER-DG P_4P_42 ($\mu = \kappa = 10^{-7}$)			
10	1.5539E-03	4.5965E-04	5.1665E-04			
20	4.3993E-05	1.0872E-05	1.0222E-05	5.14	5.40	5.66
25	1.8146E-05	4.4276E-06	4.1469E-06	3.97	4.03	4.04
30	8.6060E-06	2.1233E-06	1.9387E-06	4.09	4.03	4.17
			ADER-DG P_5P_5 ($\mu = \kappa = 10^{-7}$)			
5	1.1638E-02	1.1638E-02	1.8898E-03			
10	3.9653E-04	9.3717E-05	6.5319E-05	4.88	6.96	4.85
15	4.4638E-05	1.2572E-05	1.9056E-05	5.39	4.95	3.04
20	9.6136E-06	3.0120E-06	3.9881E-06	5.34	4.97	5.44

Blasius Boundary Layer + Poiseille Flow

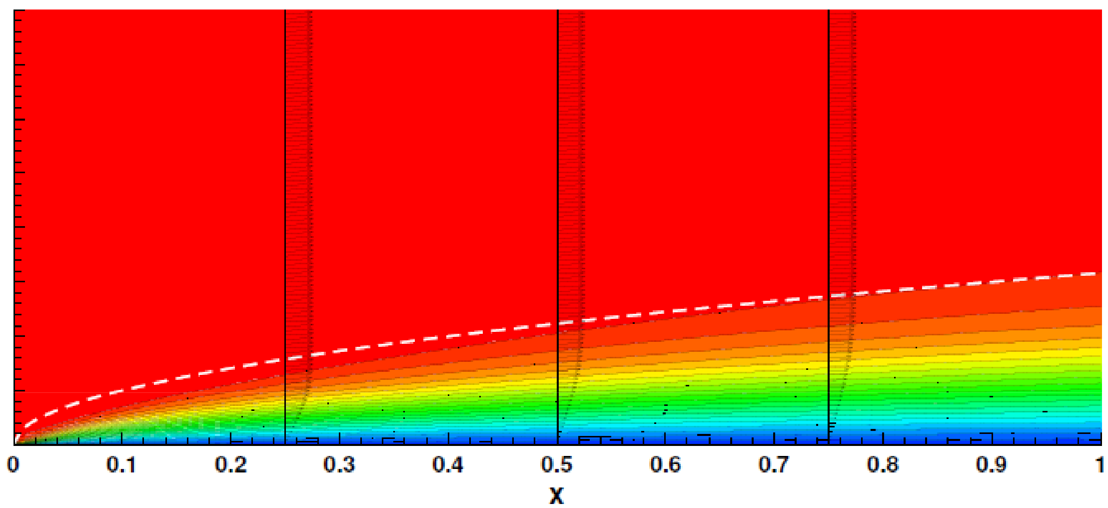

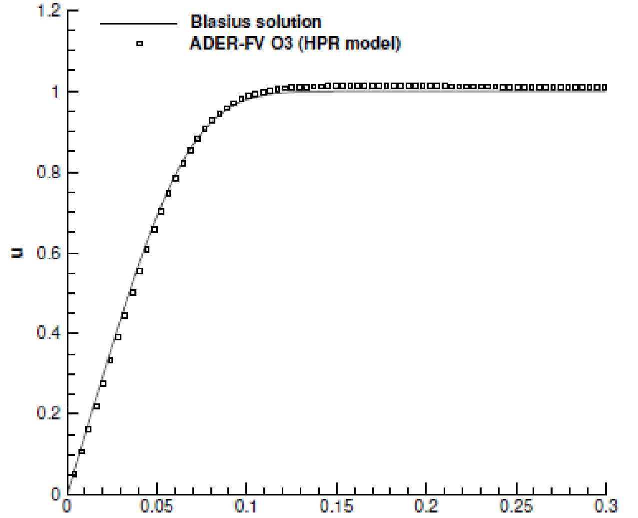

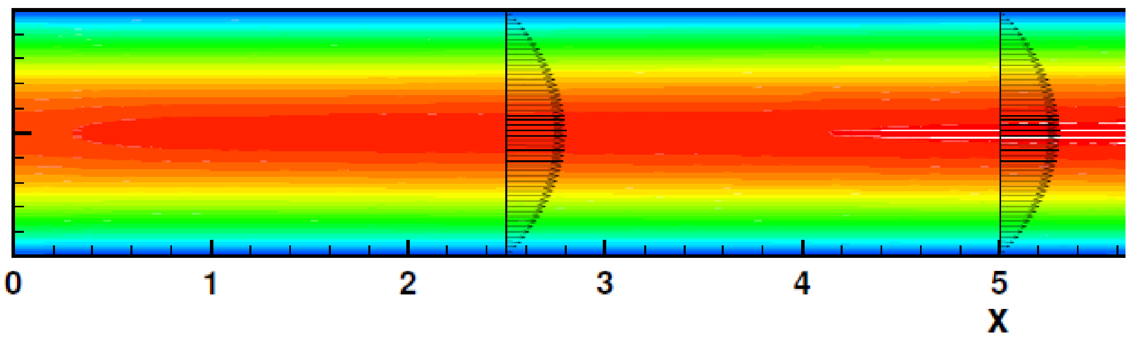

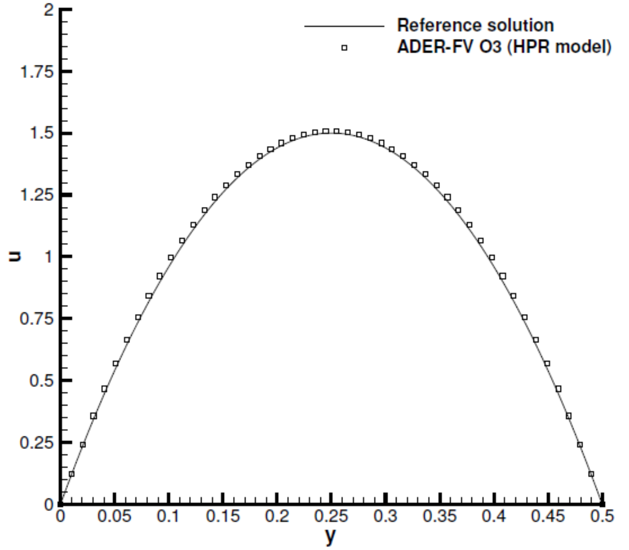

Lid-Driven Cavity Flow at Re=100

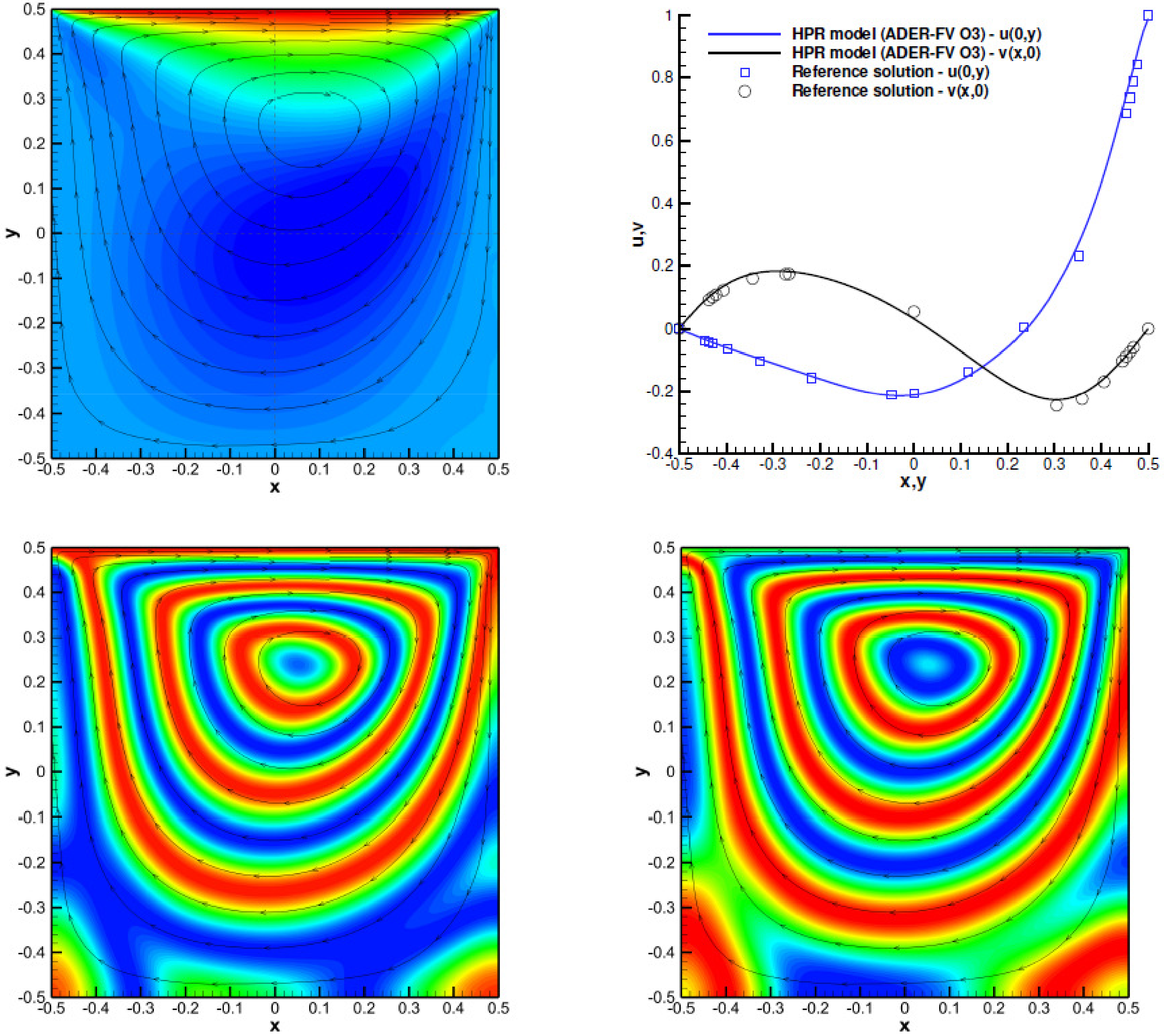

Double Shear-Layer

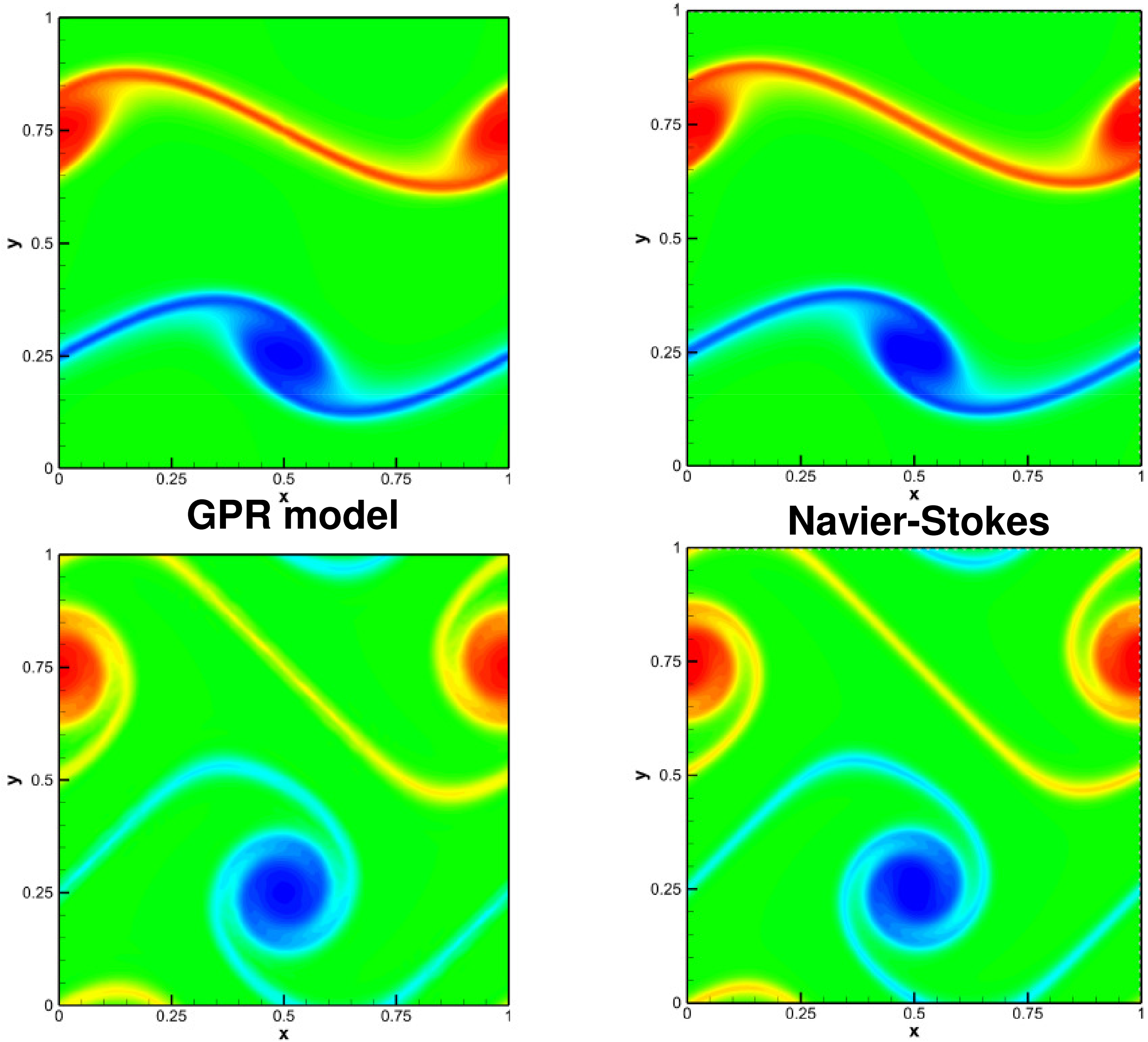

Double Shear-Layer

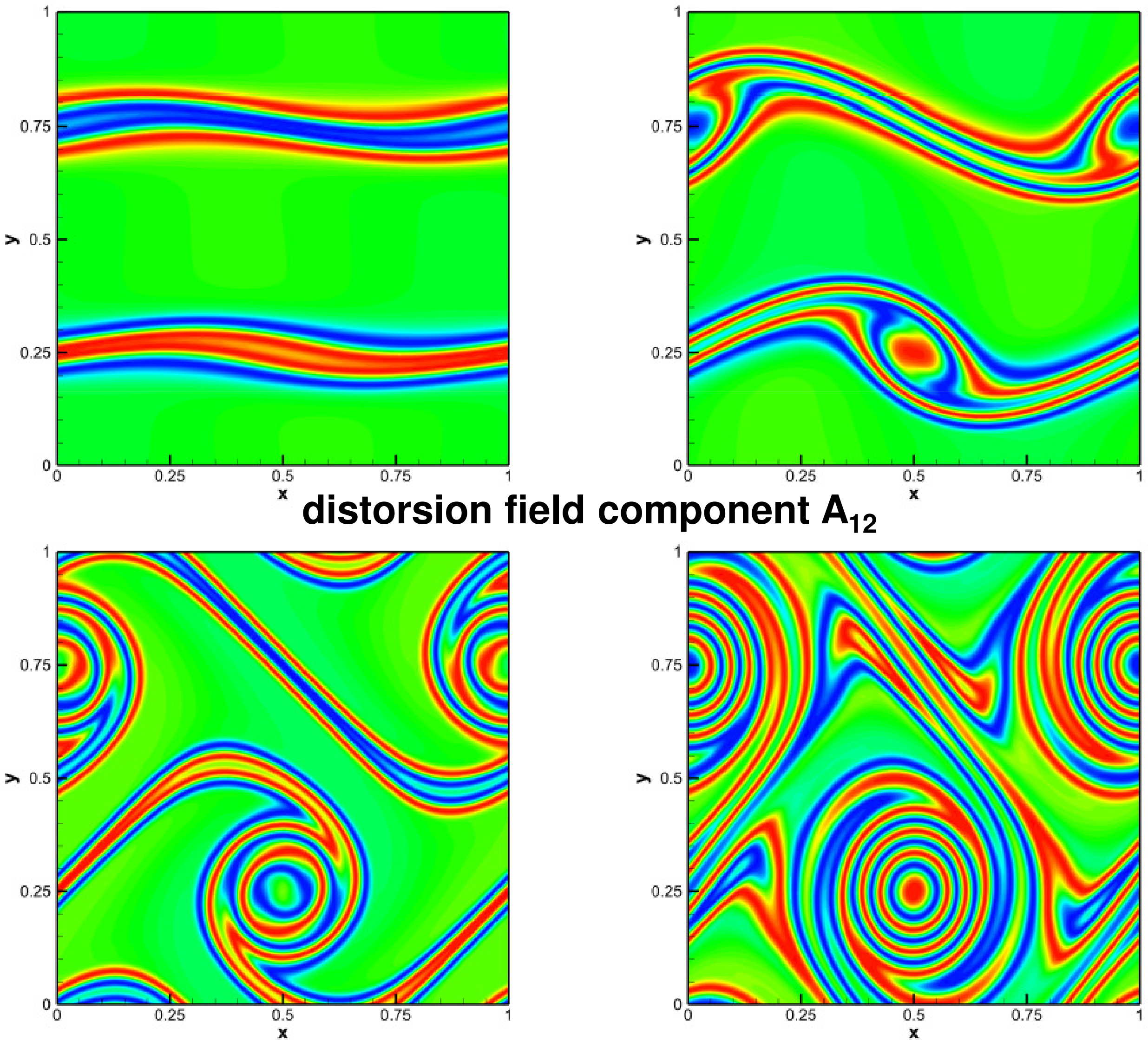

3D Taylor-Green Vortex

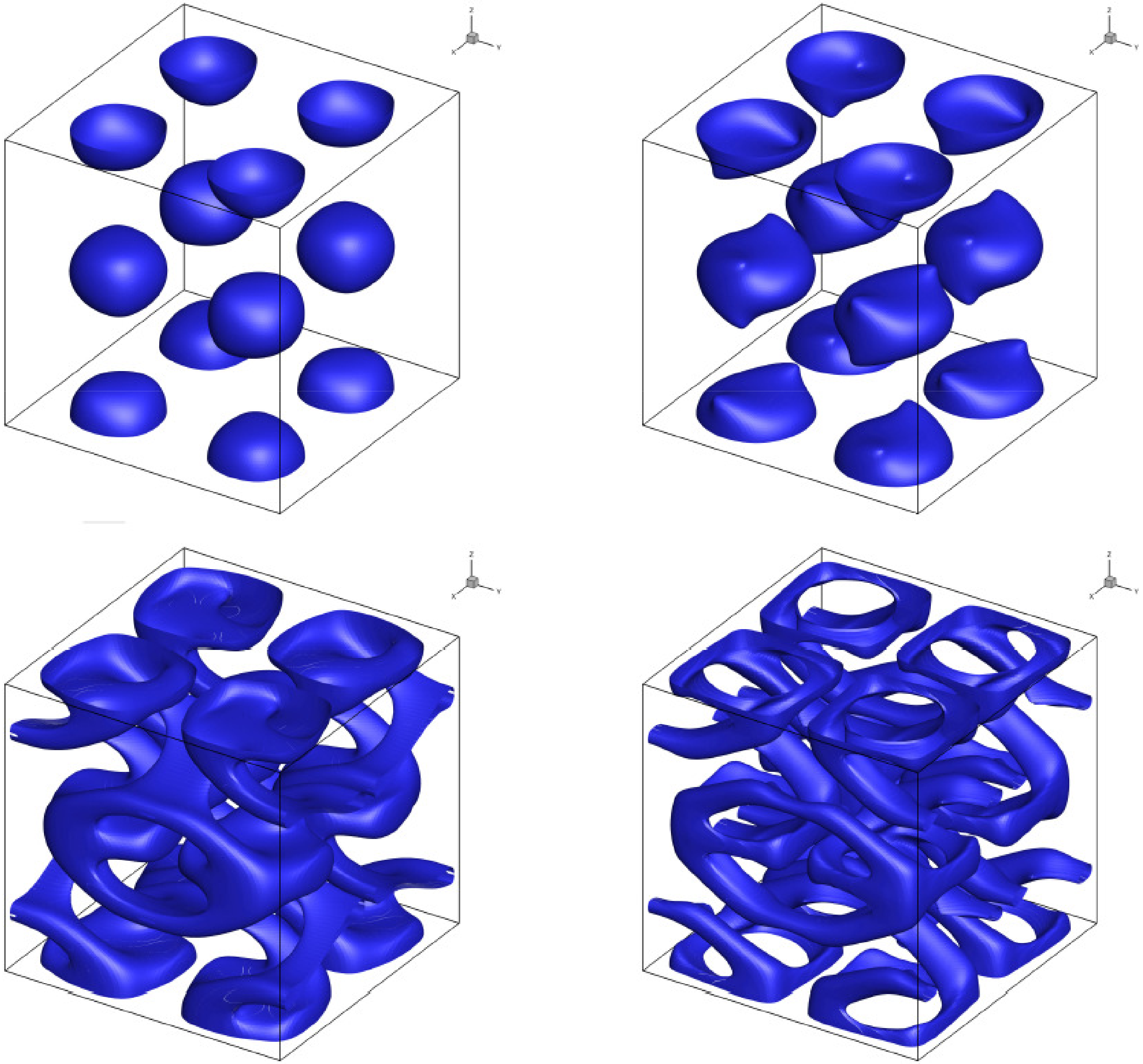

3D Taylor-Green Vortex

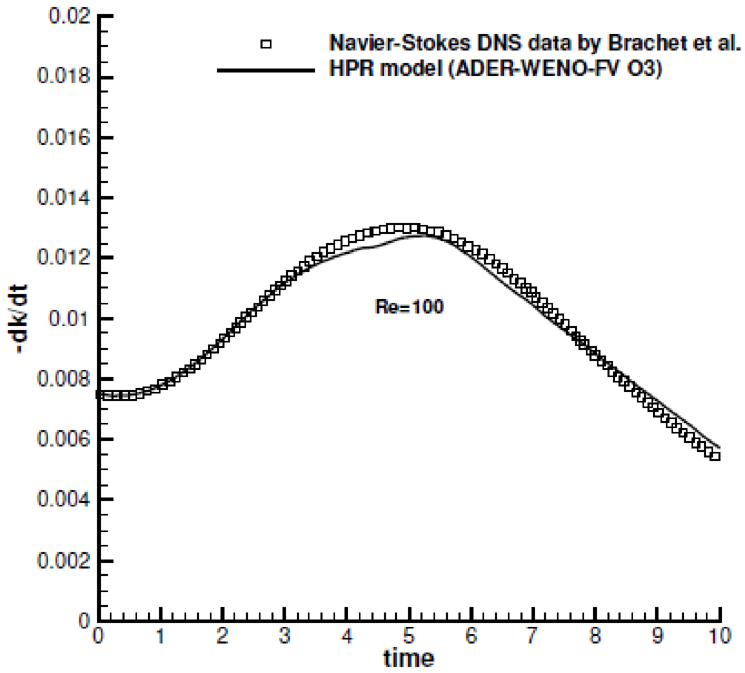

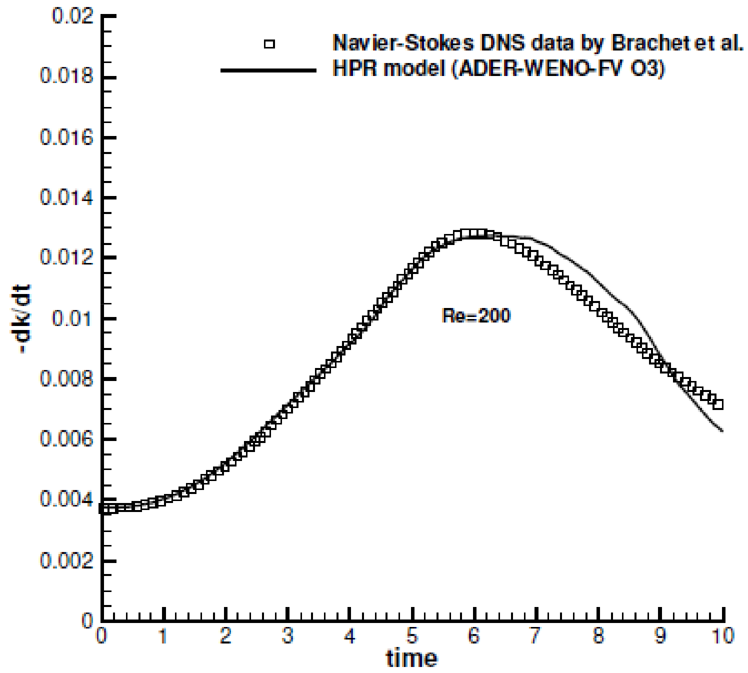

3D Taylor-Green Vortex

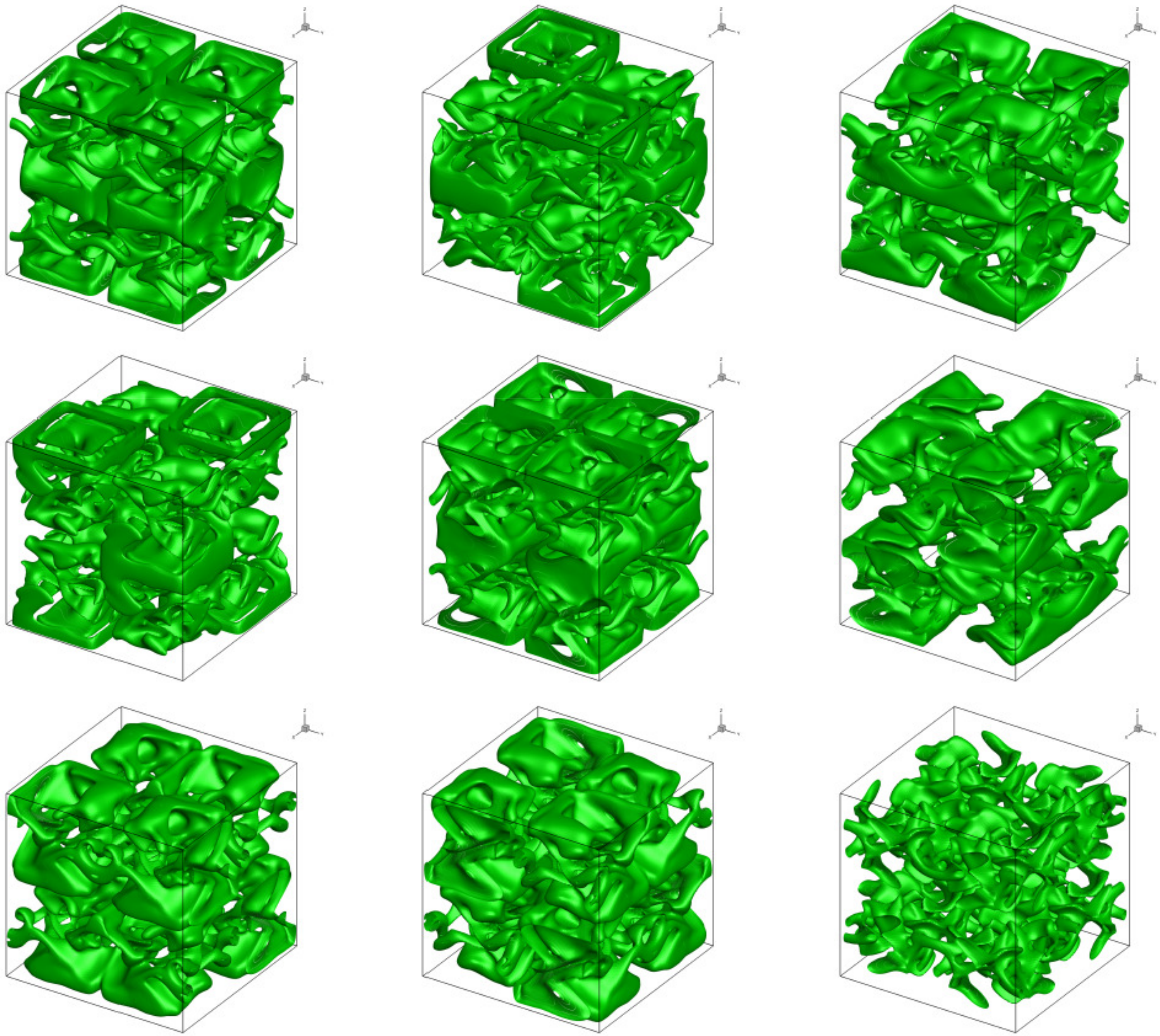

Viscous heat-conducting shock

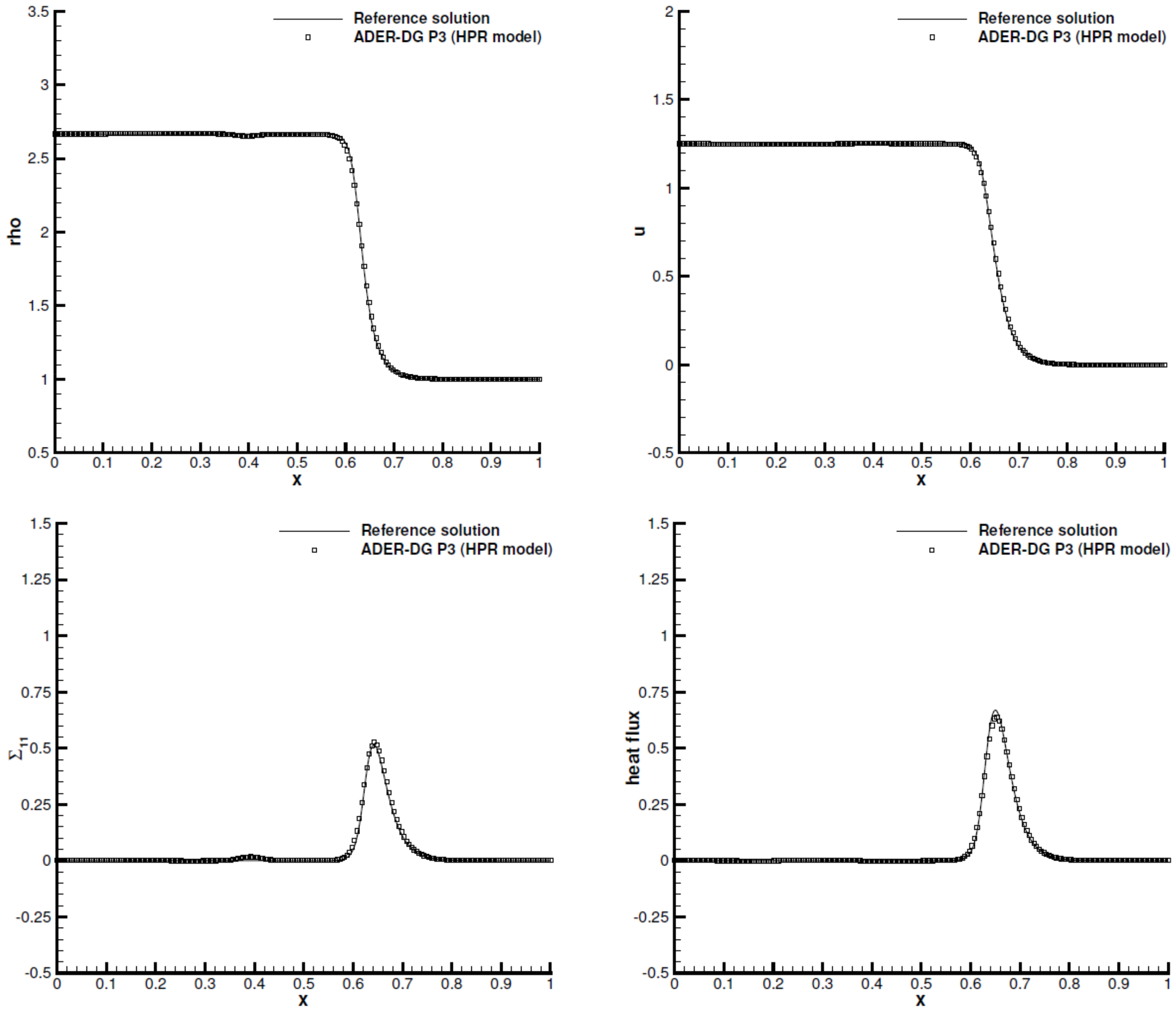

Lamb's problem from solid mechanics (simply let $\tau_1 \rightarrow \infty$)

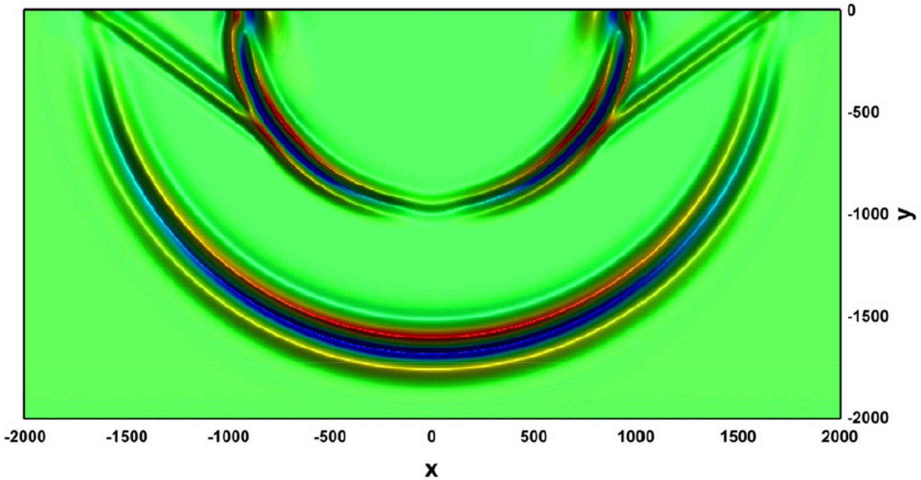

GPR model

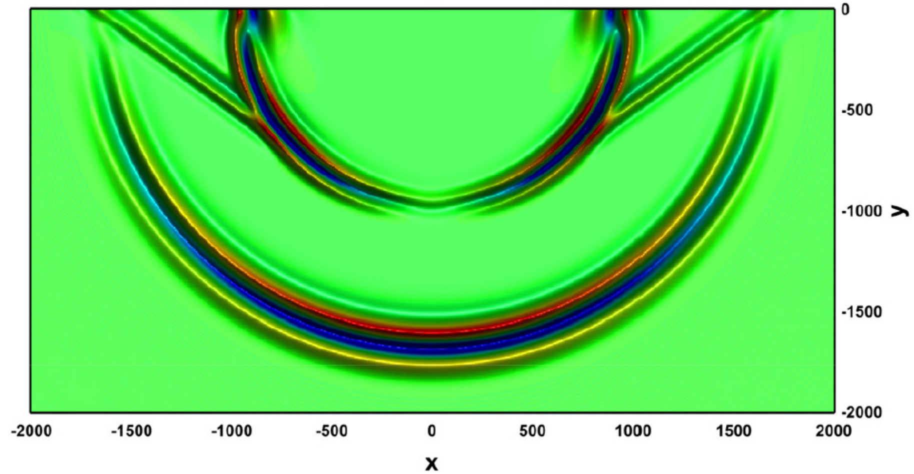

Linear elasticity

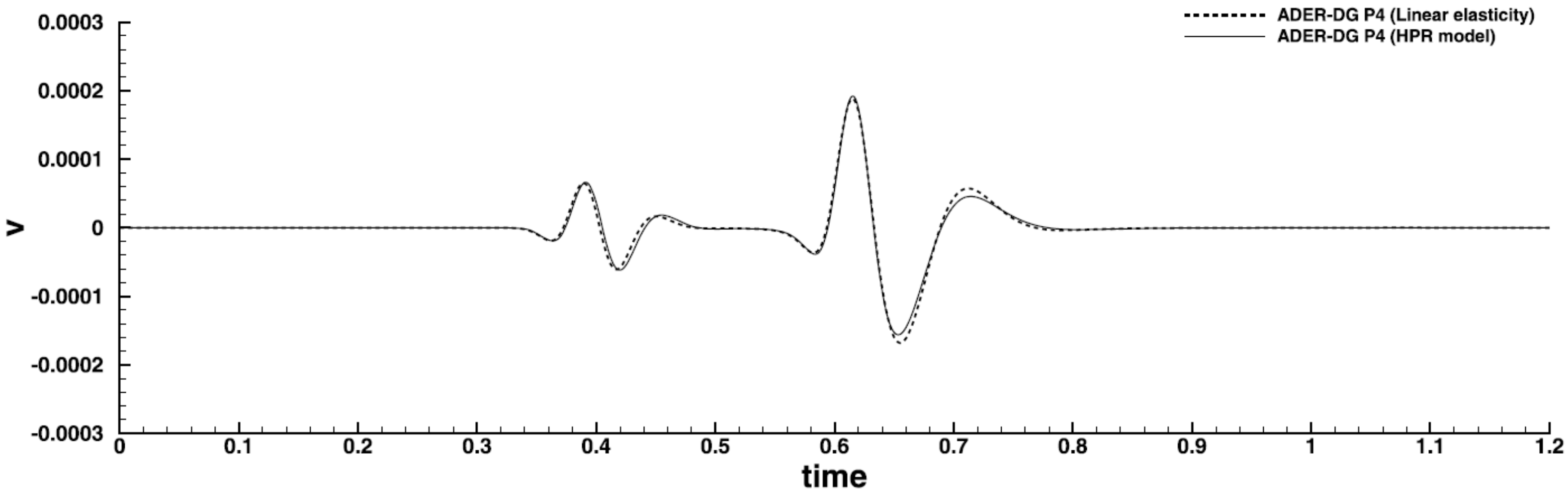

Inviscid Orszag-Tang vortex

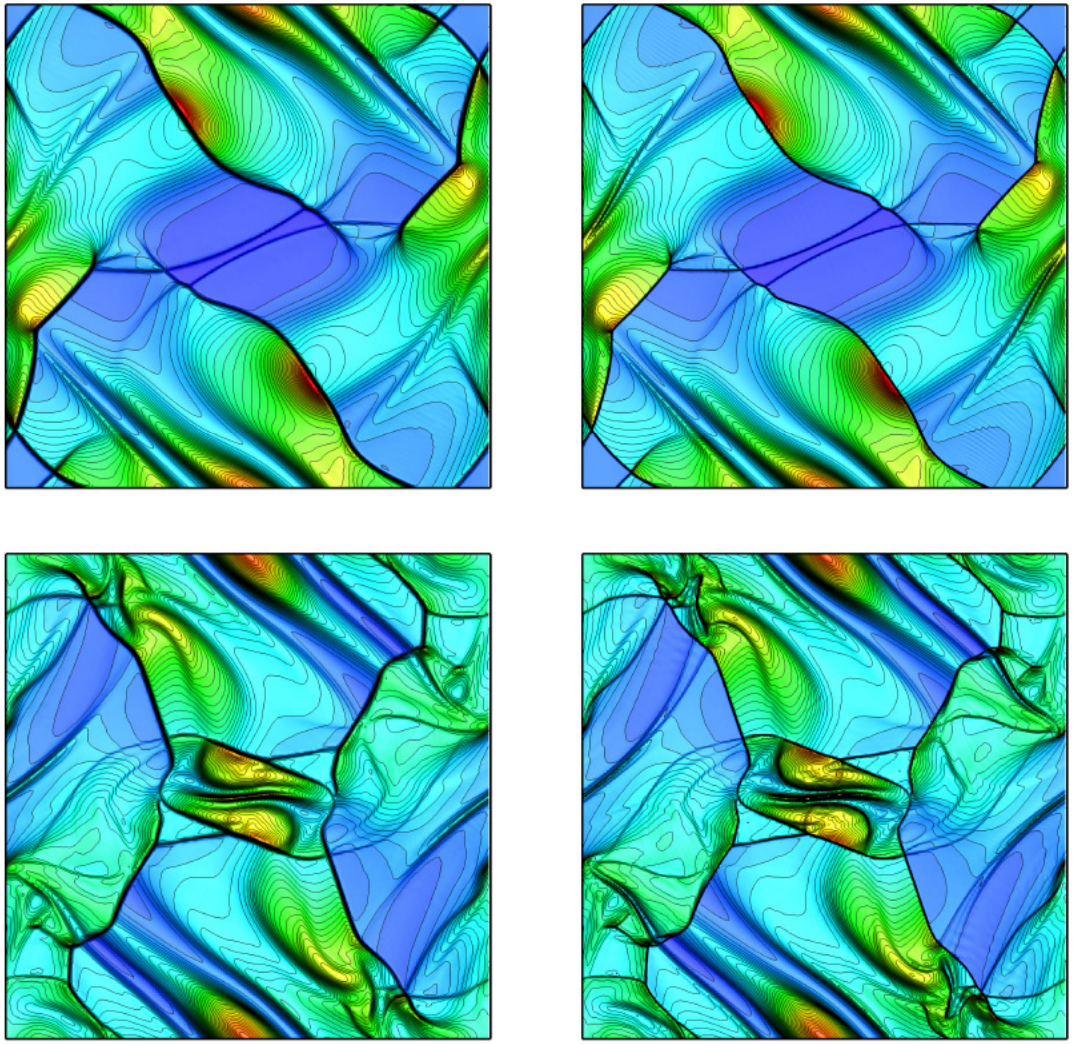

GPR model (stiff limit) **ideal MHD (inviscid)**

Viscous & resistive Orszag-Tang vortex

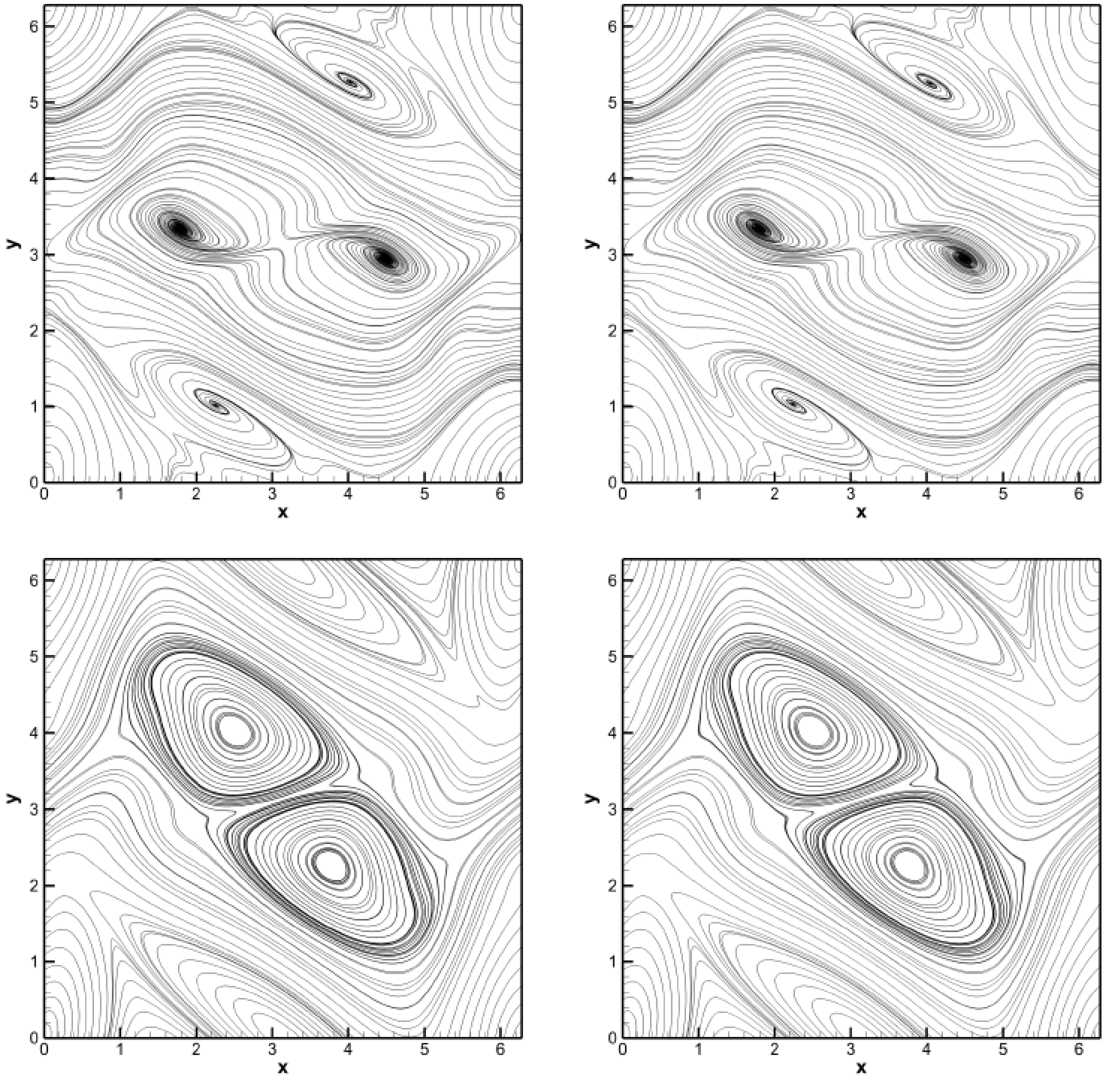

GPR model (stiff limit) **VRMHD (Re=Lu=100, Pr=1)**

Rotor problem

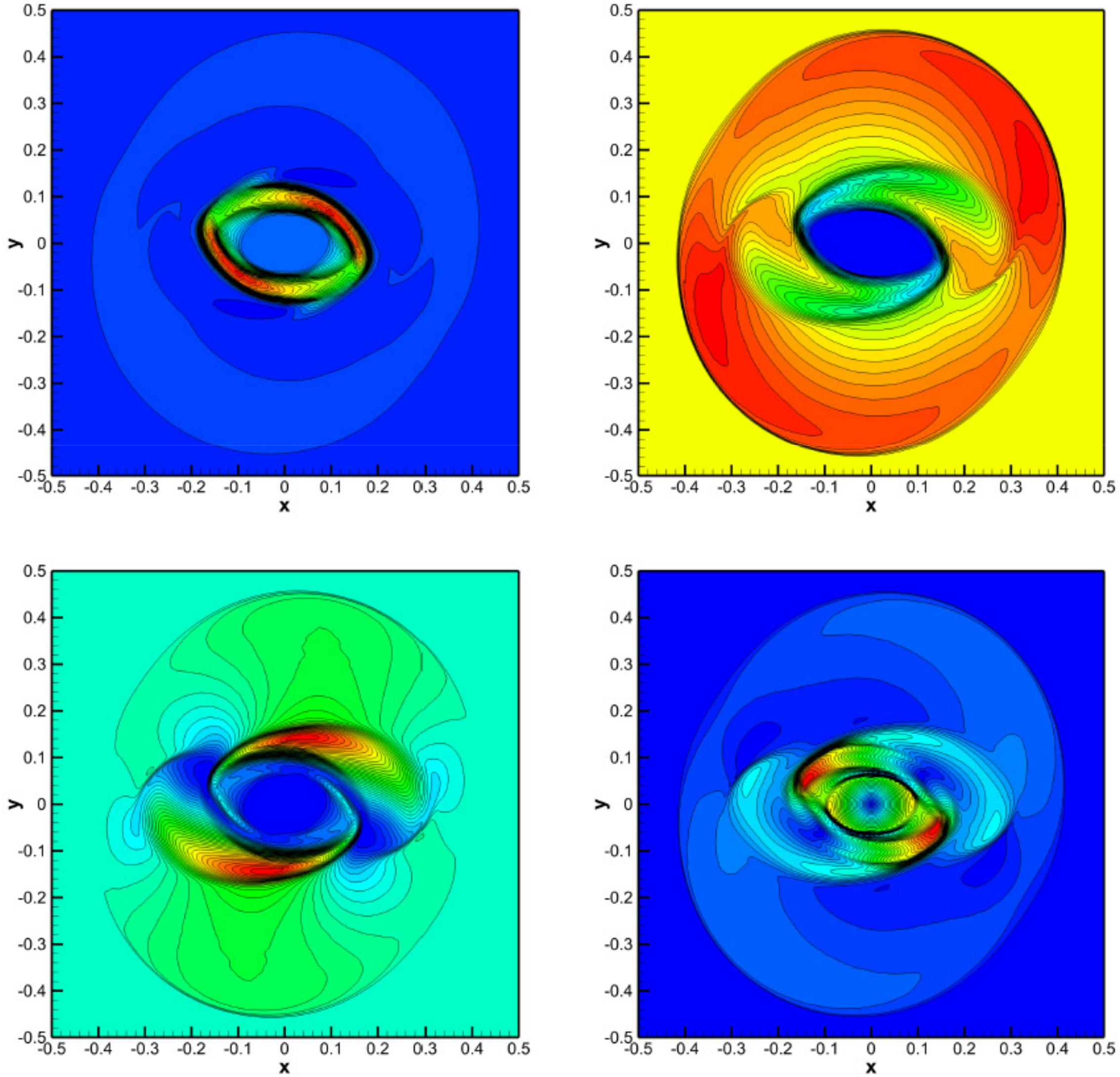

GPR model (stiff limit)

Blast wave problem

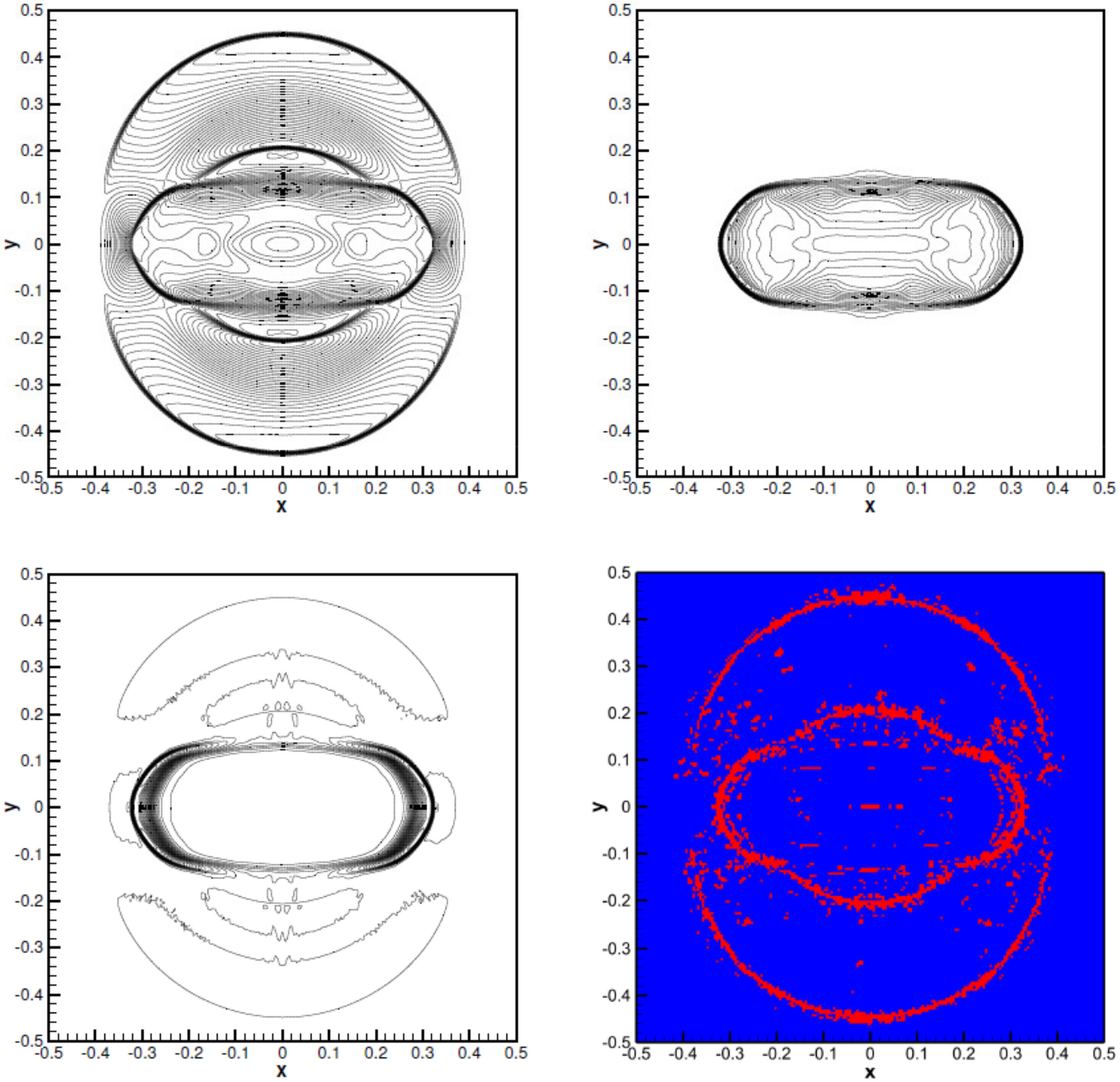

GPR model (stiff limit)

KH Instability

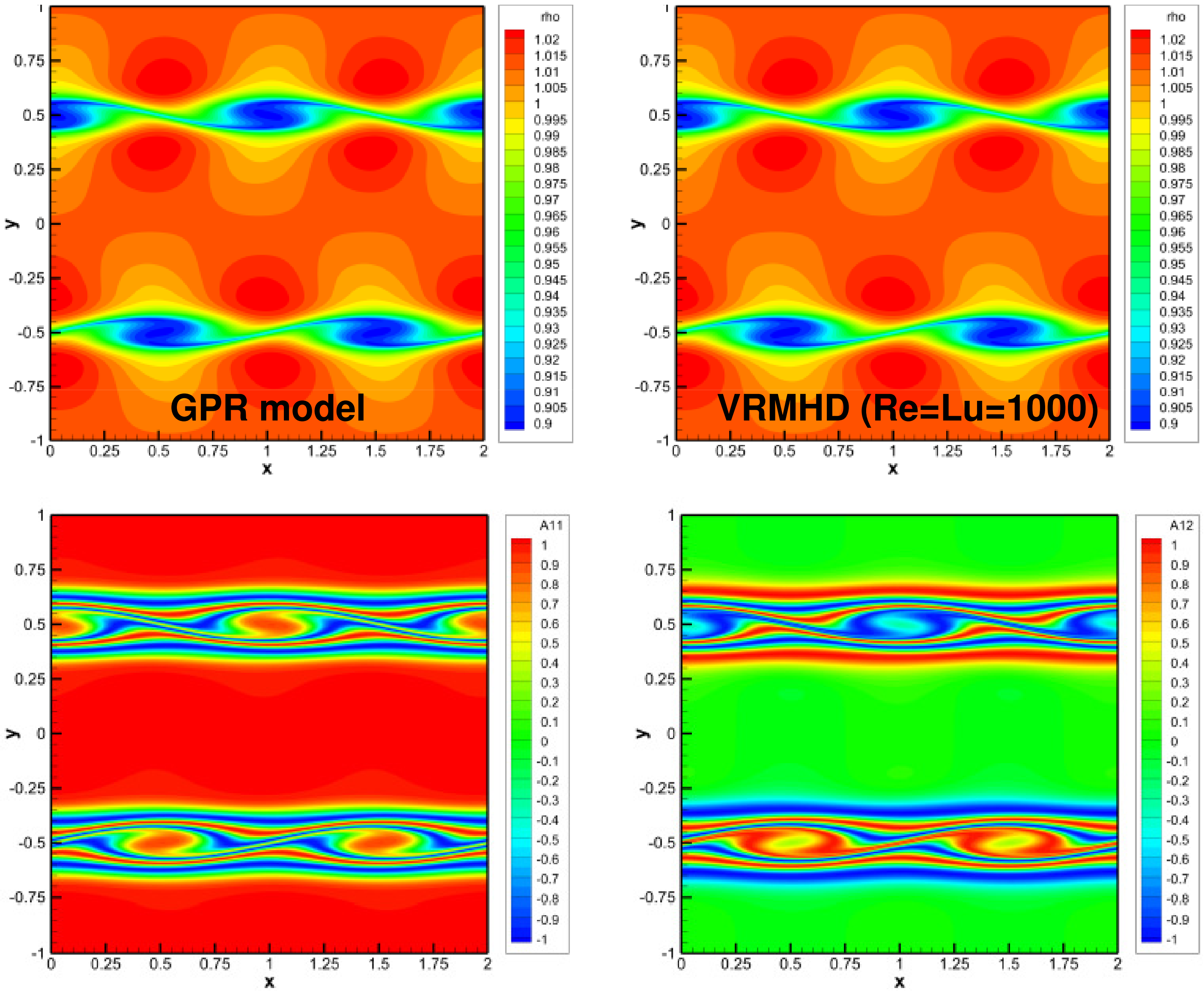

EM wave propagation in heterogeneous media

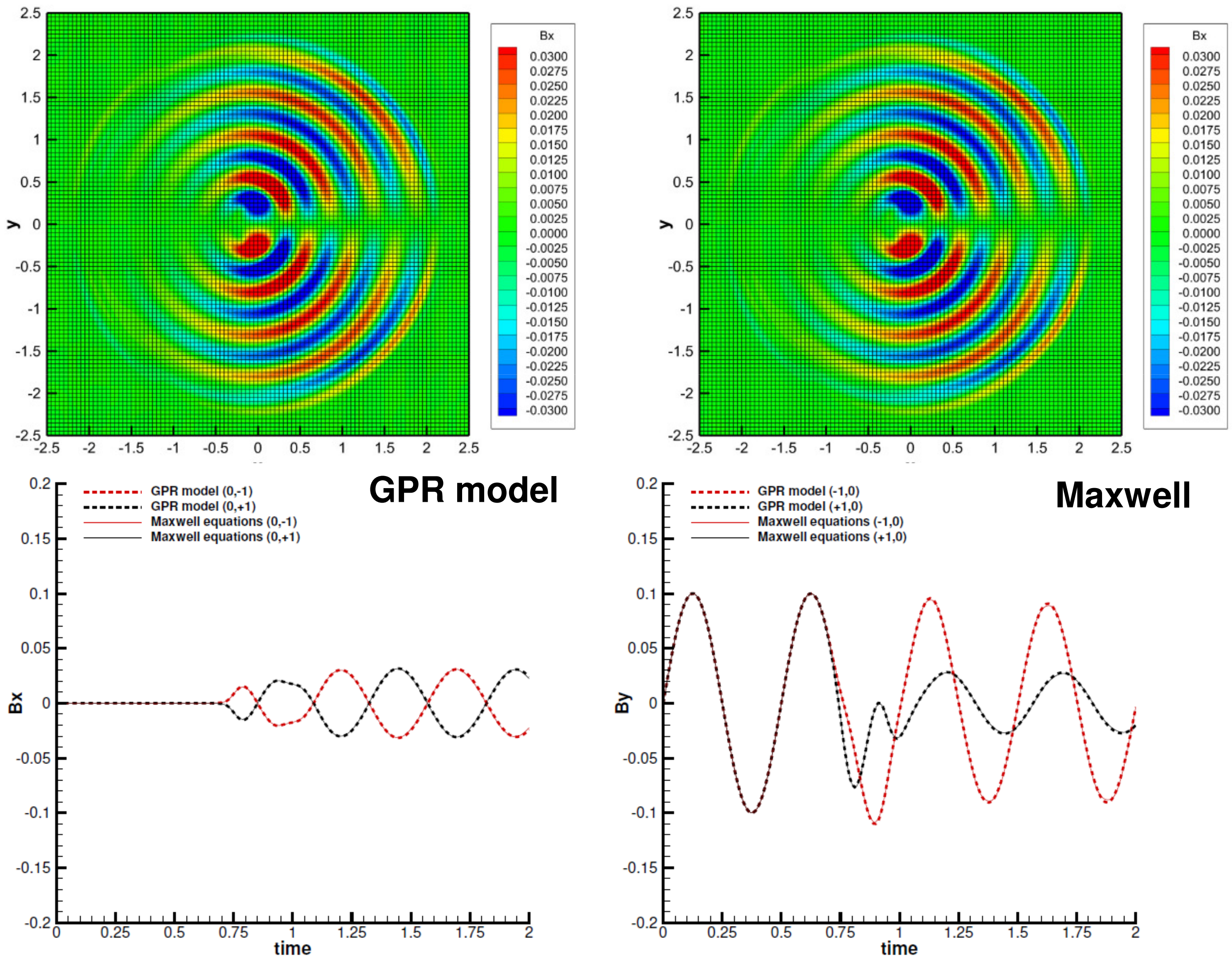

Rotor problem in different asymptotic regimes

conducting fluid

conducting solid

non-conducting solid

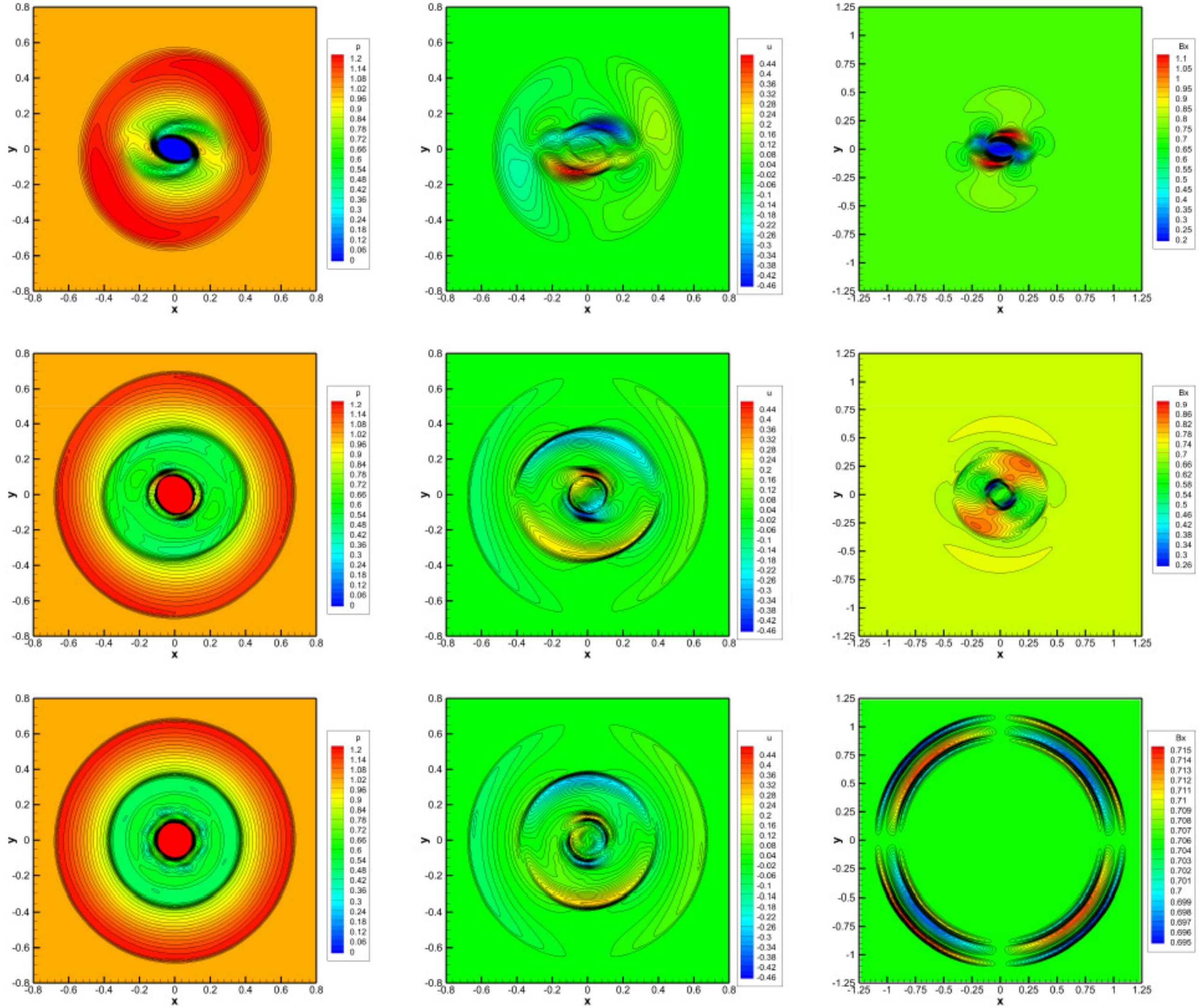

General relativistic GPR model (4D form)

$$\nabla_\mu J^\mu = 0$$

$$\nabla_\nu T^{\mu\nu} = 0$$

$$u^\kappa \left(\nabla_\kappa A^i{}_\mu - \nabla_\mu A^i{}_\kappa \right) = -\frac{1}{\tau\theta} k^{ij} g_{\mu\nu} \epsilon_{A^j{}_\nu}$$

$$\nabla_\mu (s u^\mu) = \frac{1}{\epsilon_s \theta \tau} k^{ij} g_{\mu\nu} \epsilon_{A^i{}_\mu} \epsilon_{A^j{}_\nu} \geq 0$$

$$J^\mu = \rho u^\mu$$

$$T^{\mu\nu} = \rho h u^\mu u^\nu + p g^{\mu\nu} + \sigma^{\mu\nu}$$

$$\rho h = \rho + \rho\epsilon + p$$

The GRGPR model requires only a *rather minor modification of existing RHD codes!*

General relativistic GPR model (3+1 form)

$$\partial_t \left(\gamma^{\frac{1}{2}} D\right) + \partial_i \left[\gamma^{\frac{1}{2}} D \left(\alpha v^i - \beta^i\right)\right] = 0$$

$$\partial_t \left(\gamma^{\frac{1}{2}} S_j\right) + \partial_i \left[\gamma^{\frac{1}{2}} \left(\alpha S^i{}_j - \beta^i S_j\right)\right] - \gamma^{\frac{1}{2}} \left(\frac{1}{2} \alpha S^{ik} \partial_j \gamma_{ik} + S_i \partial_j \beta^i - E \partial_j \alpha\right) = 0$$

$$\partial_t \left(\gamma^{\frac{1}{2}} \tau\right) + \partial_i \left[\gamma^{\frac{1}{2}} \left(\alpha \left(S^i - D v^i\right) - \tau \beta^i\right)\right] - \gamma^{\frac{1}{2}} \left(\alpha S^{ij} K_{ij} - S^j \partial_j \alpha\right) = 0$$

$$\partial_t A^i{}_k + \partial_k \left(\hat{v}^m A^i{}_m\right) + \hat{v}^j \left(\partial_j A^i{}_k - \partial_k A^i{}_j\right) = -\frac{1}{\tau \theta} A^i{}_\mu dev G^\mu_k$$

$$\partial_t k_{AB} + \hat{v}^k \partial_k k_{AB} = 0$$

$$\partial_t \alpha = 0$$

$$\partial_t \beta_j = 0$$

$$\partial_t \gamma_{ij} = 0$$

The structure of the kinematic equation for the geometric object *A* is exactly the same as in the Newtonian limit! This is a rather remarkable property.

The GRGPR model requires only *very minor modifications of existing RHD codes!*

General relativistic GPR model

$$S^i{}_j = \rho h W^2 v^i v_j + p\gamma^i_j + \sigma^i{}_j \qquad \sigma^{ij} := \gamma^i_\alpha \gamma^j_\beta \sigma^{\alpha\beta}$$

$$S_i = \rho h W^2 v_i + \sigma_i, \qquad \sigma_i := -\gamma_{i\alpha} n_\beta \sigma^{\alpha\beta}$$

$$E = \rho h W^2 - p + \sigma \qquad \sigma := n_\alpha n_\beta \sigma^{\alpha\beta}$$

$$G^\mu_\nu = g^{\mu\lambda} k_{AB} A^A_\lambda A^B_\nu$$

$$\breve{G}_{\mu\nu} := G_{\mu\nu} - \frac{G^\lambda_\lambda}{3} h_{\mu\nu}$$

$$\varepsilon(A^i{}_\mu, \rho, s) = \varepsilon^{\mathrm{eq}}(\rho, s) + \frac{c_s^2}{4} \breve{G}^\lambda{}_\nu \breve{G}^\nu{}_\lambda$$

$$\sigma_{\mu\nu} = g_{\mu\alpha}\sigma^\alpha{}_\nu = g_{\mu\alpha} A^M{}_\nu \epsilon_{A^M_\alpha} = \rho\, c_s^2 \breve{G}_{\mu\lambda} G^\lambda{}_\nu.$$

The GRGPR model requires only a *rather minor modification of existing RHD codes!*

General relativistic GPR model

- The GRGPR model is *covariant* and *causal*, with finite signal speeds for all processes, including dissipative ones!

- The mathematical structure of the evolution equations for the distortion field ***A*** is identical with the Newtonian equations, which is very remarkable!

- The formula for the 4D stress tensor is formally identical to the Newtonian formula!

- The GRGPR model describes elastic solids as well as viscous and inviscid fluids!

- In the asymptotic limit, the stress tensor of the GRGPR model tends to the viscous stress tensor conjectured by Landau. Here, it is a result of the GRGPR model, it has never been explicitly put into the model !

$$-\sigma_{\mu\nu} = \kappa^{(0)}\tau\theta\frac{1}{2}\left(\nabla_\nu u_\mu + \nabla_\mu u_\nu + u^\lambda\nabla_\lambda(u_\mu u_\nu) - \frac{2}{3}(h^{\alpha\lambda}\nabla_\lambda u_\alpha)h_{\mu\nu}\right)$$

$$\mu = \frac{1}{2}\tau\theta\kappa^{(0)} = \frac{1}{6}\rho\tau c_s^2. \qquad \tau \to 0$$

General relativistic GPR model

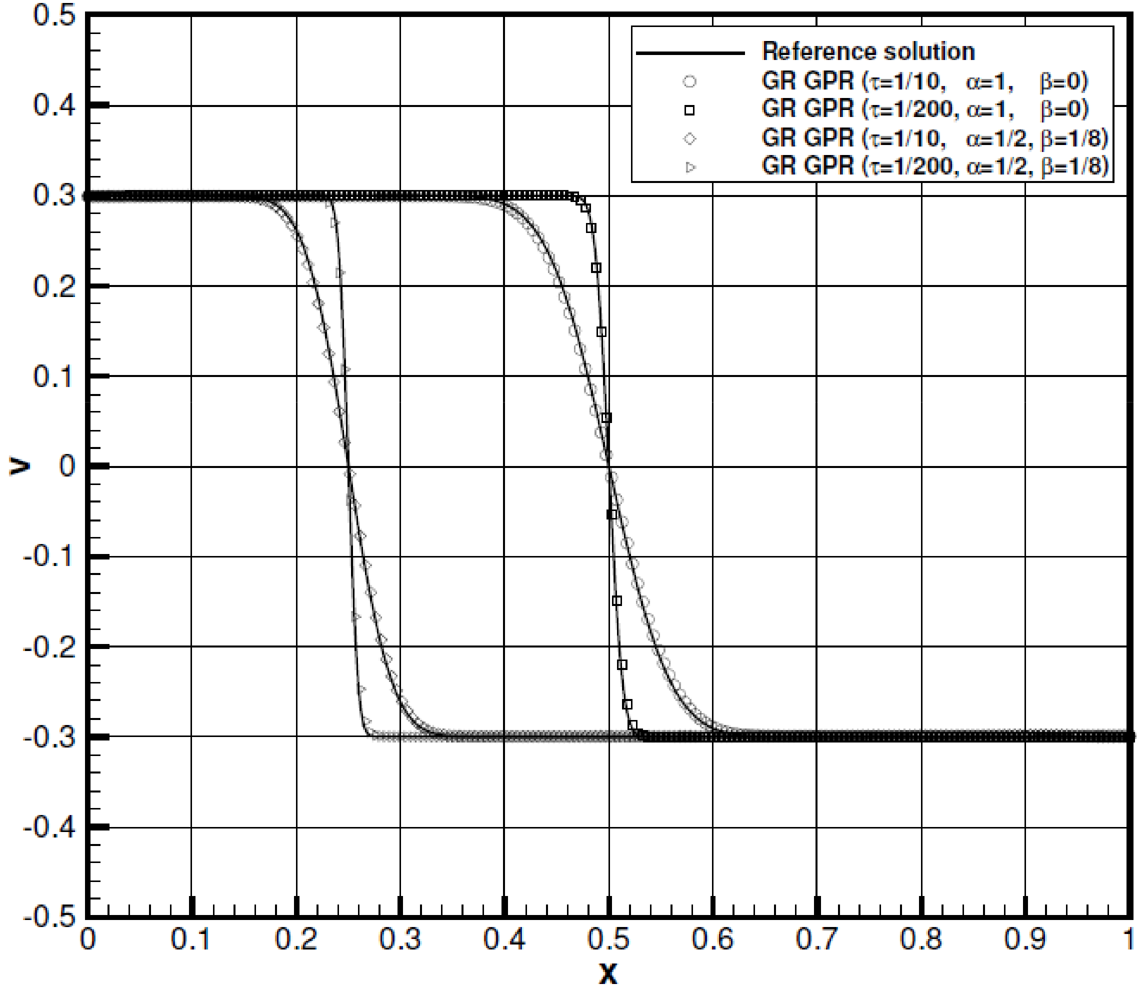

Shear layer (viscous fluid)

General relativistic GPR model

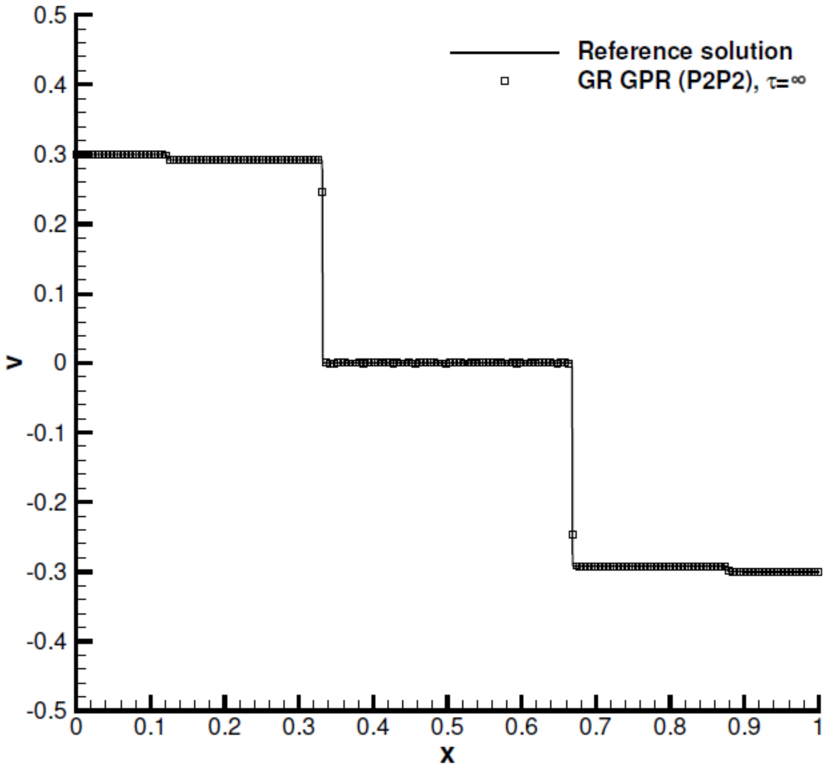

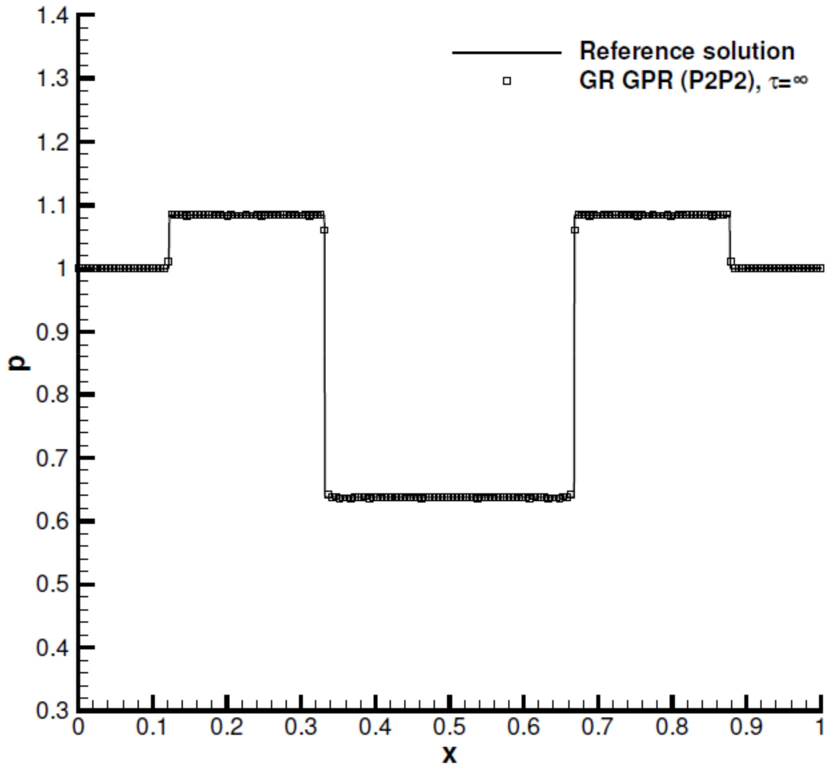

Shear layer (ideal elastic solid)

General relativistic GPR model

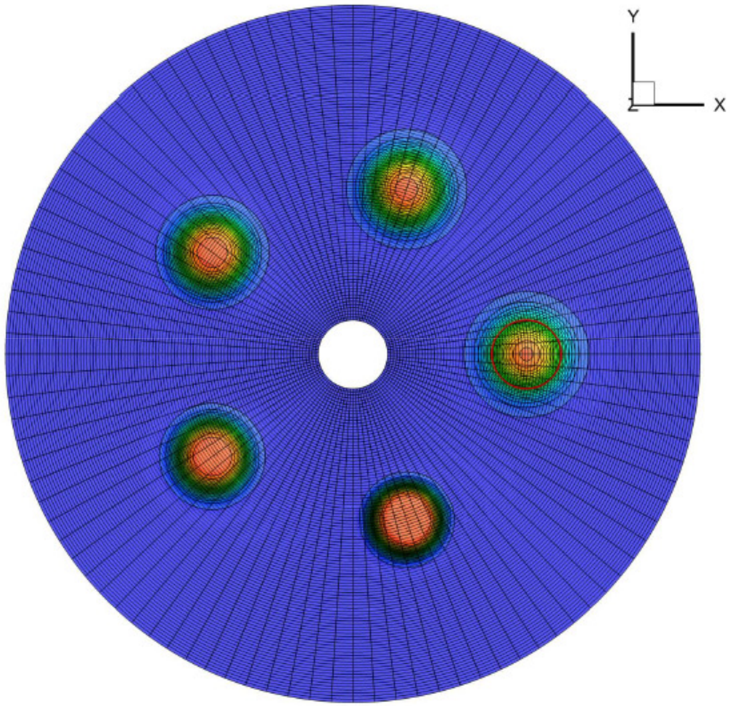

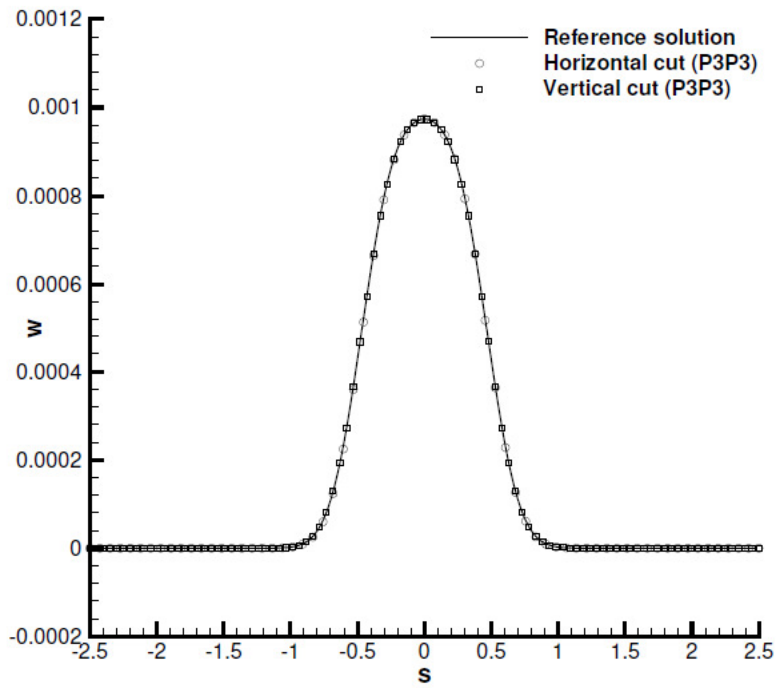

Shear flow (viscous fluid) in a *moving curvilinear* coordinate system (the computational grid is Cartesian and fixed, of course).

General relativistic GPR model

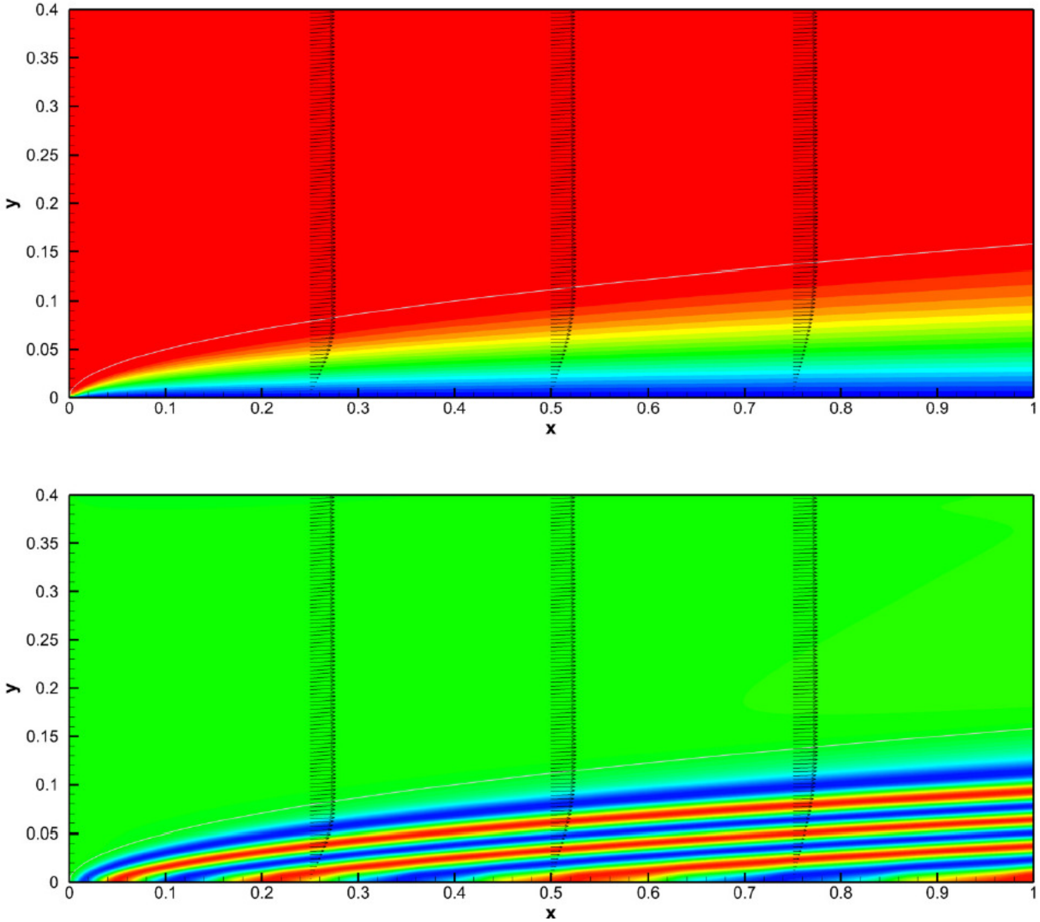

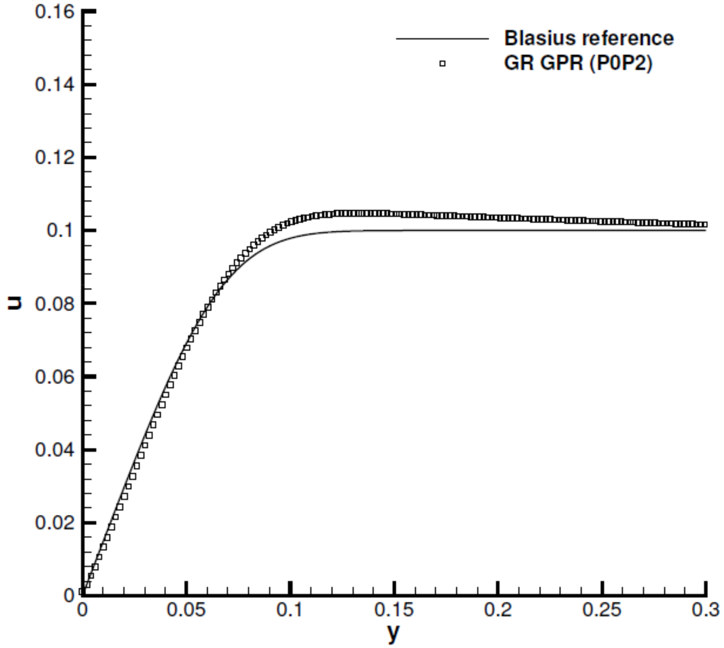

Laminar boundary layer flow over a flat plate.

General relativistic GPR model

coarse grid

fine grid

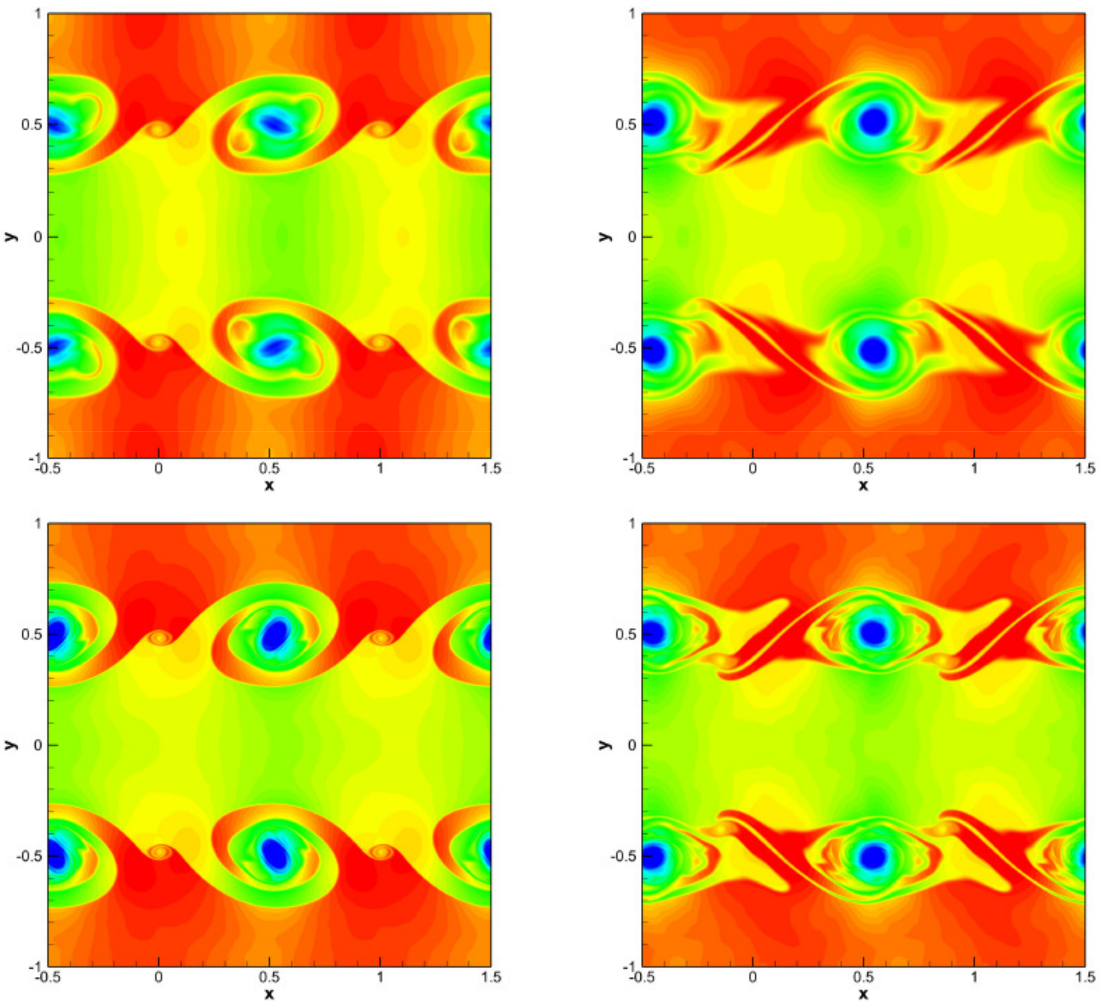

<u>Inviscid</u> Kelvin-Helmholtz instability. <u>Ideal</u> RHD equations.
Results are <u>not</u> grid independent.

General relativistic GPR model

coarse grid

fine grid

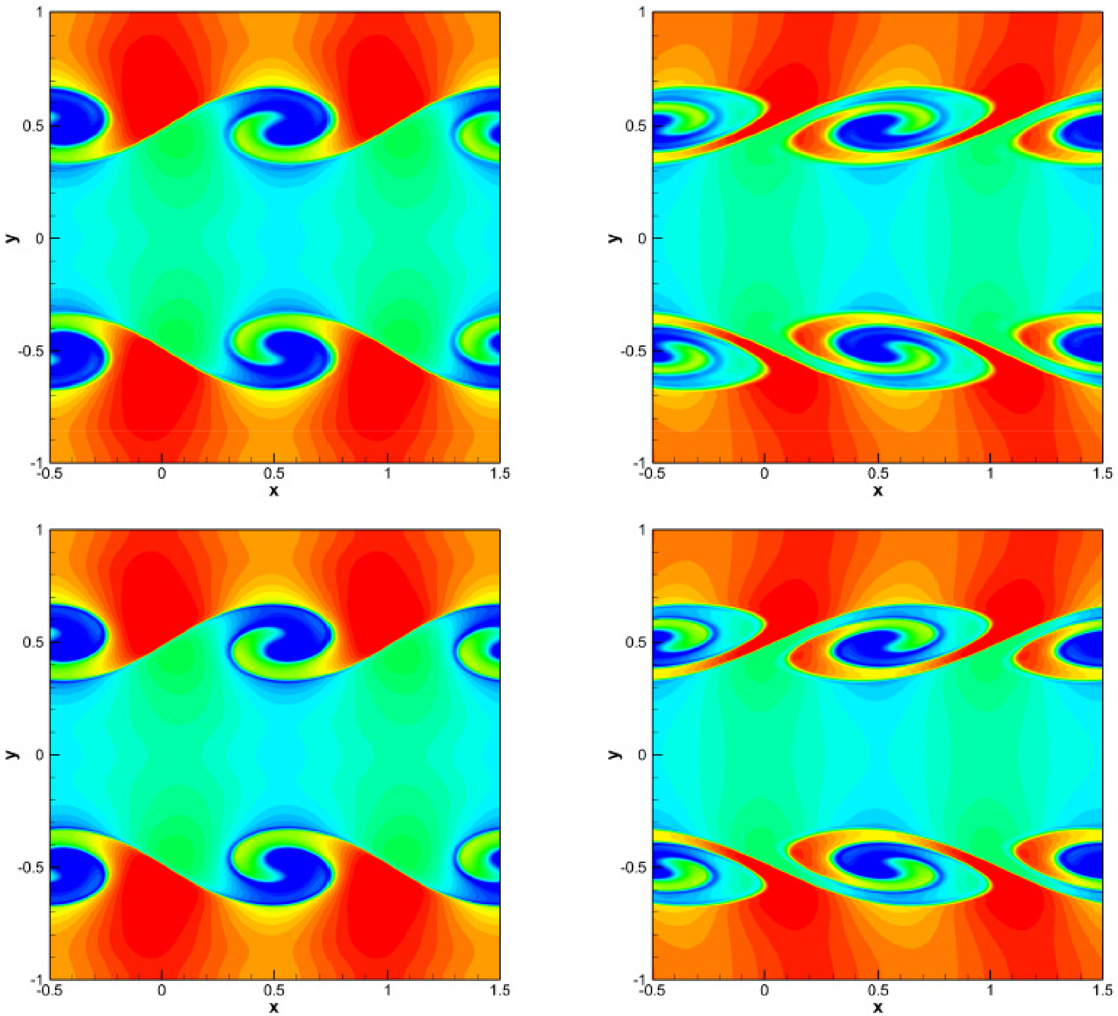

Viscous Kelvin-Helmholtz instability. New GRGPR model.
Results are grid independent! Will allow DNS of viscous relativsitic flows.

General relativistic GPR model

coarse grid

fine grid

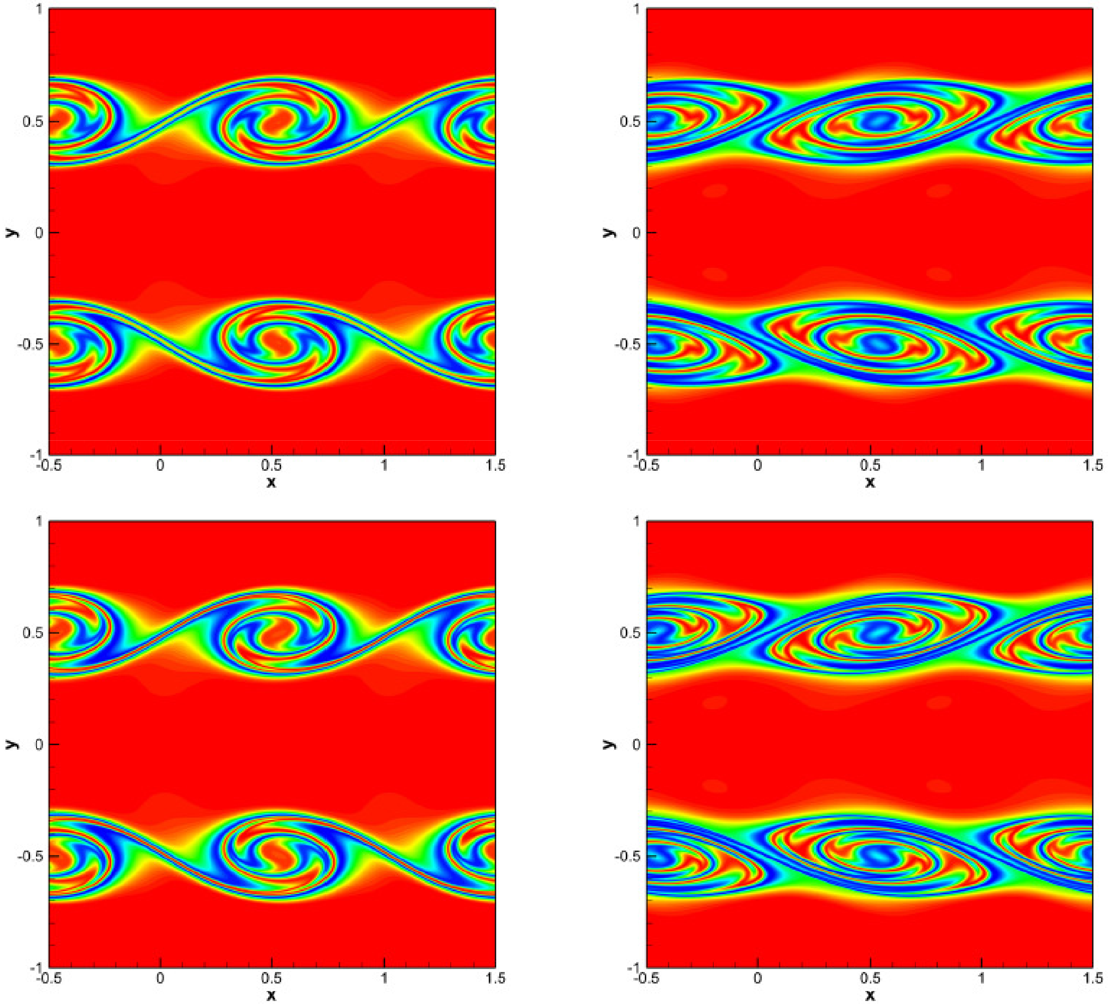

Viscous Kelvin-Helmholtz instability. New **GRGPR** model.
Contour colors of the distortion field component A_{11}

General relativistic GPR model

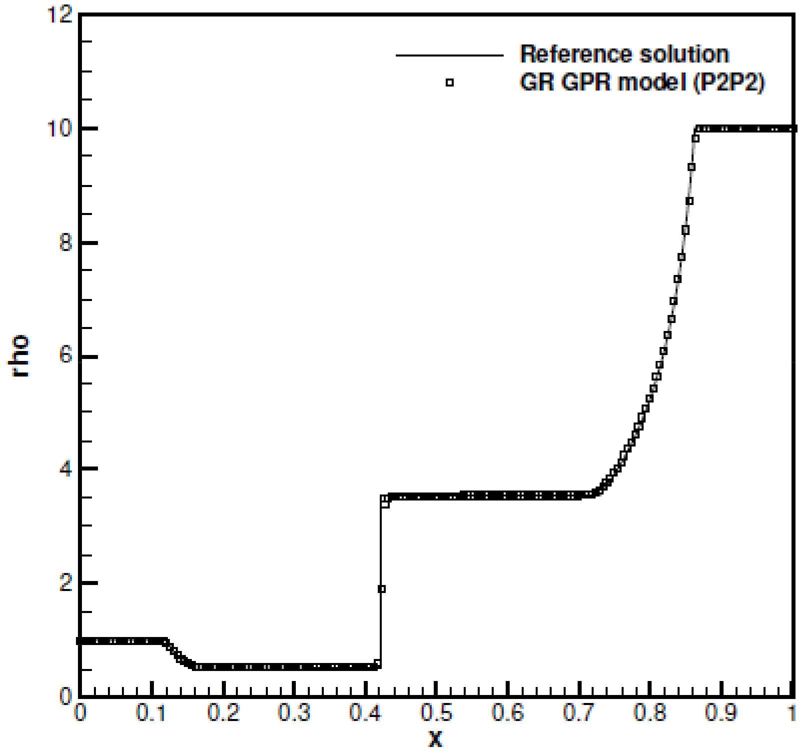

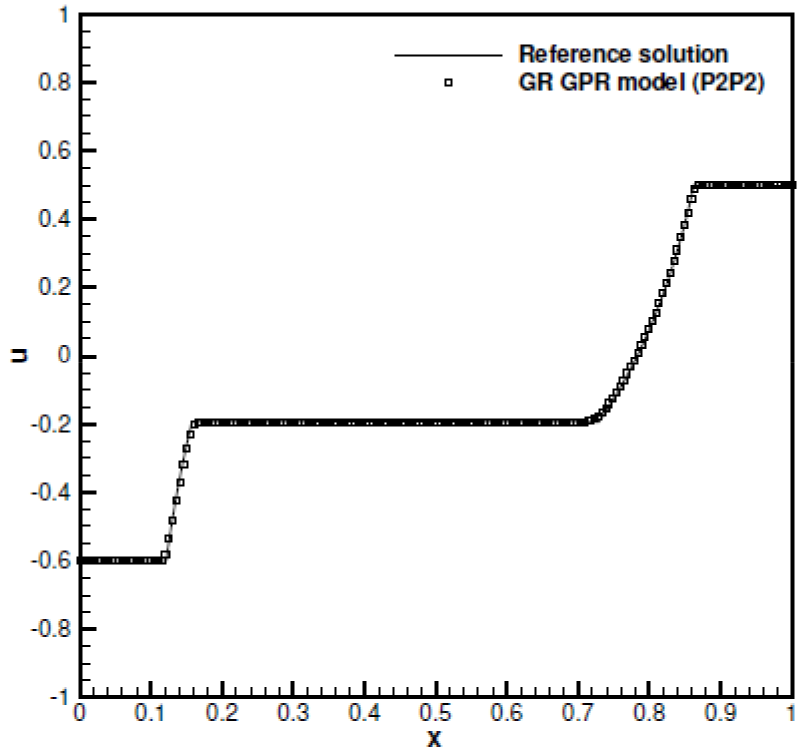

In the stiff relaxation limit, we recover the ideal RHD equations.
Comparison with the exact solution of the RHD equations for some Riemann problems.

General relativistic GPR model

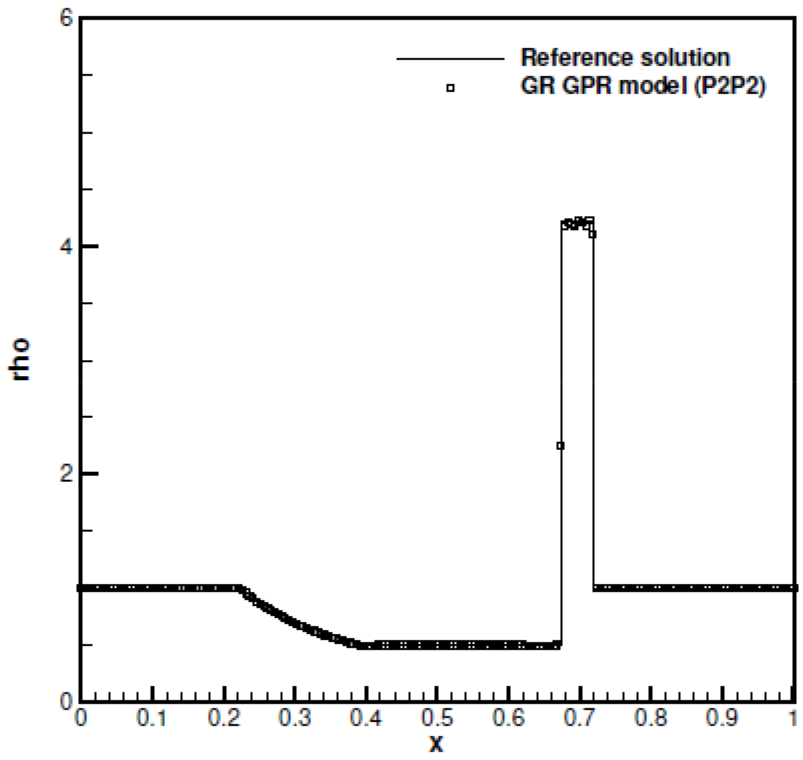

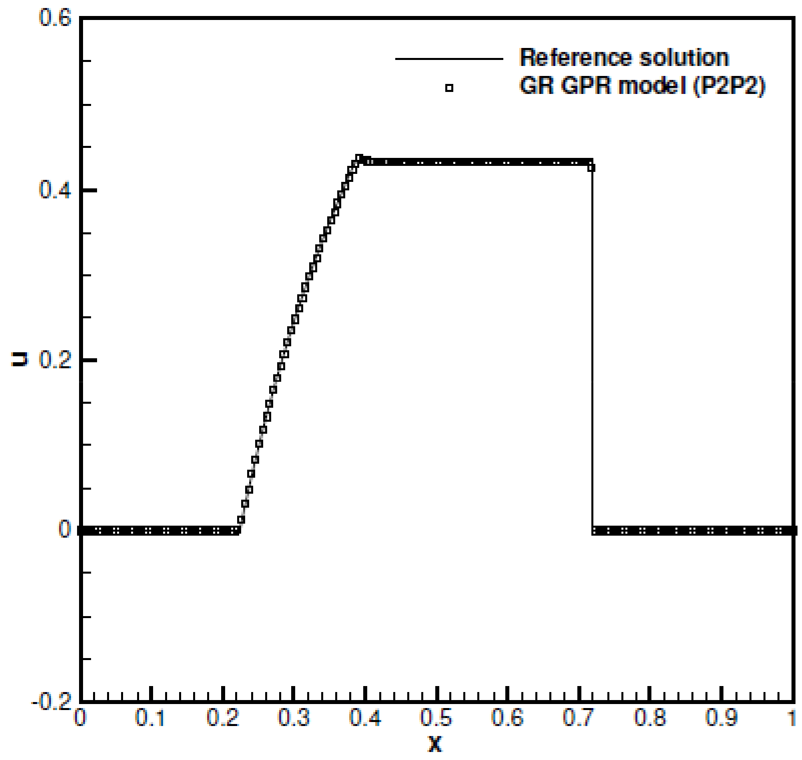

In the stiff relaxation limit, we recover the ideal RHD equations.
Comparison with the exact solution of the RHD equations for some Riemann problems.

General relativistic GPR model

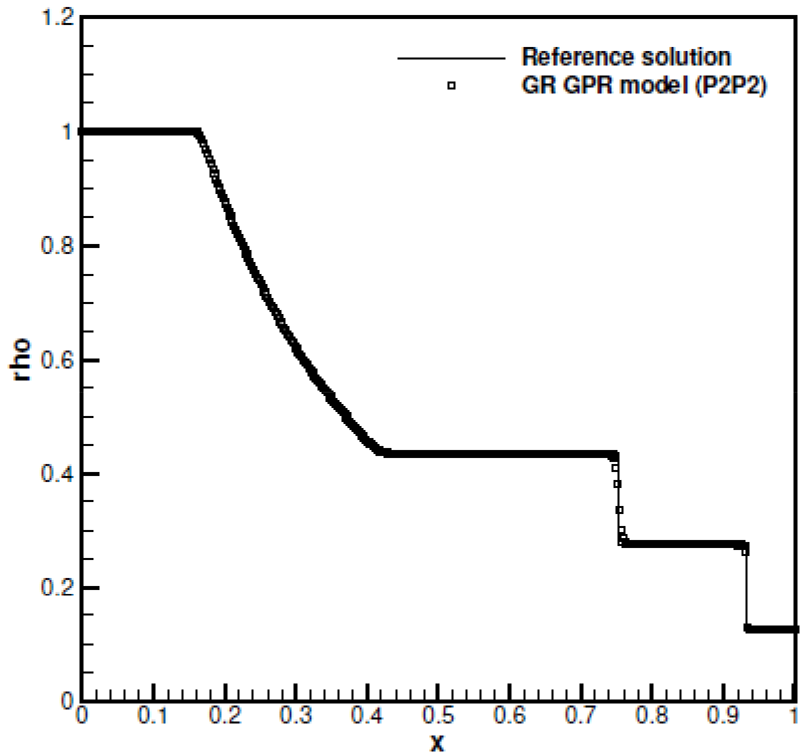

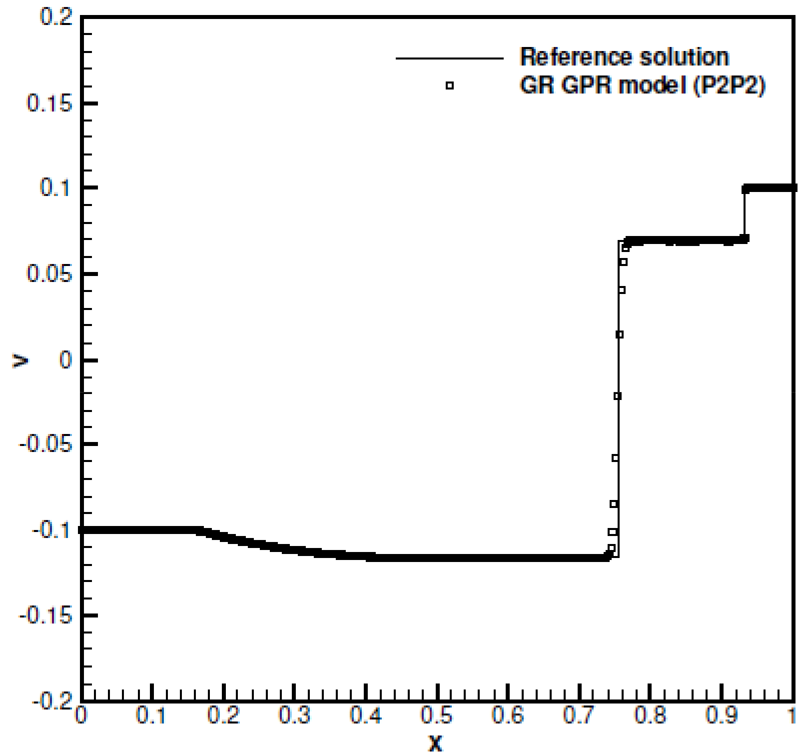

In the stiff relaxation limit, we recover the ideal RHD equations.
Comparison with the exact solution of the RHD equations for some Riemann problems.

General relativistic GPR model

Fluid limit
$\tau \rightarrow 0$

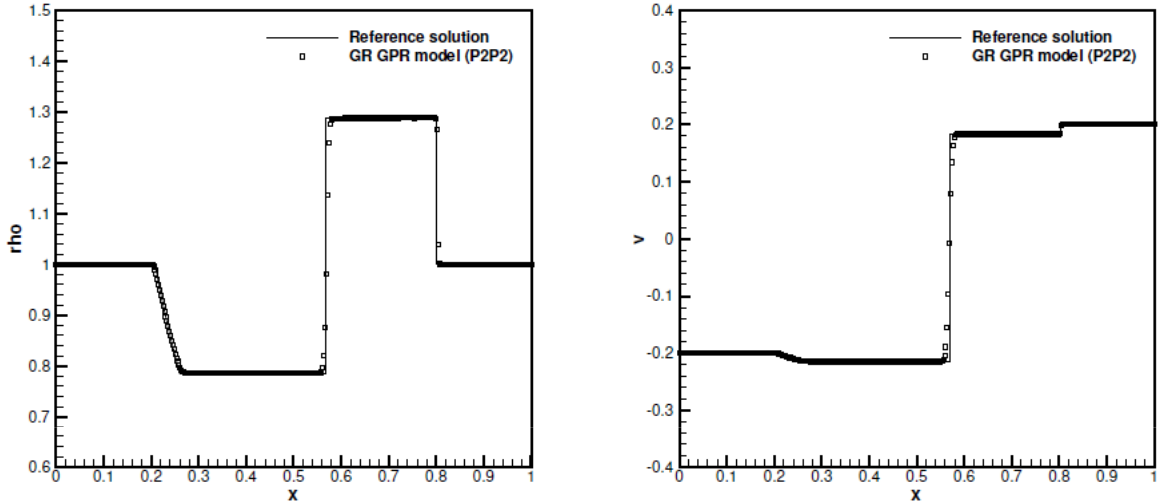

Elastic solid
$\tau \rightarrow \infty$

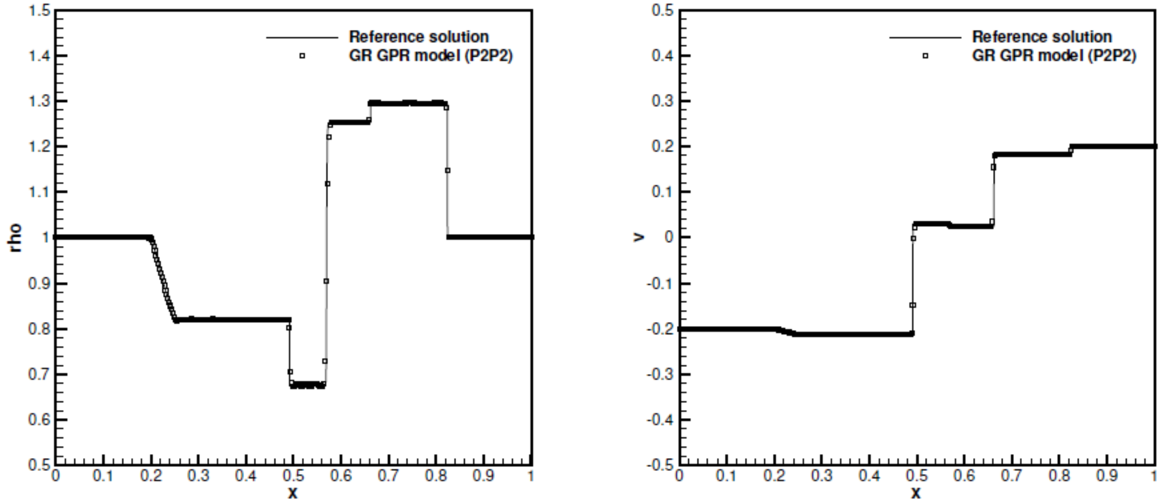

Direct comparison of the two relaxation limits of the GRGPR model. Fluid (top) and elastic solid (bottom)

General relativistic GPR model

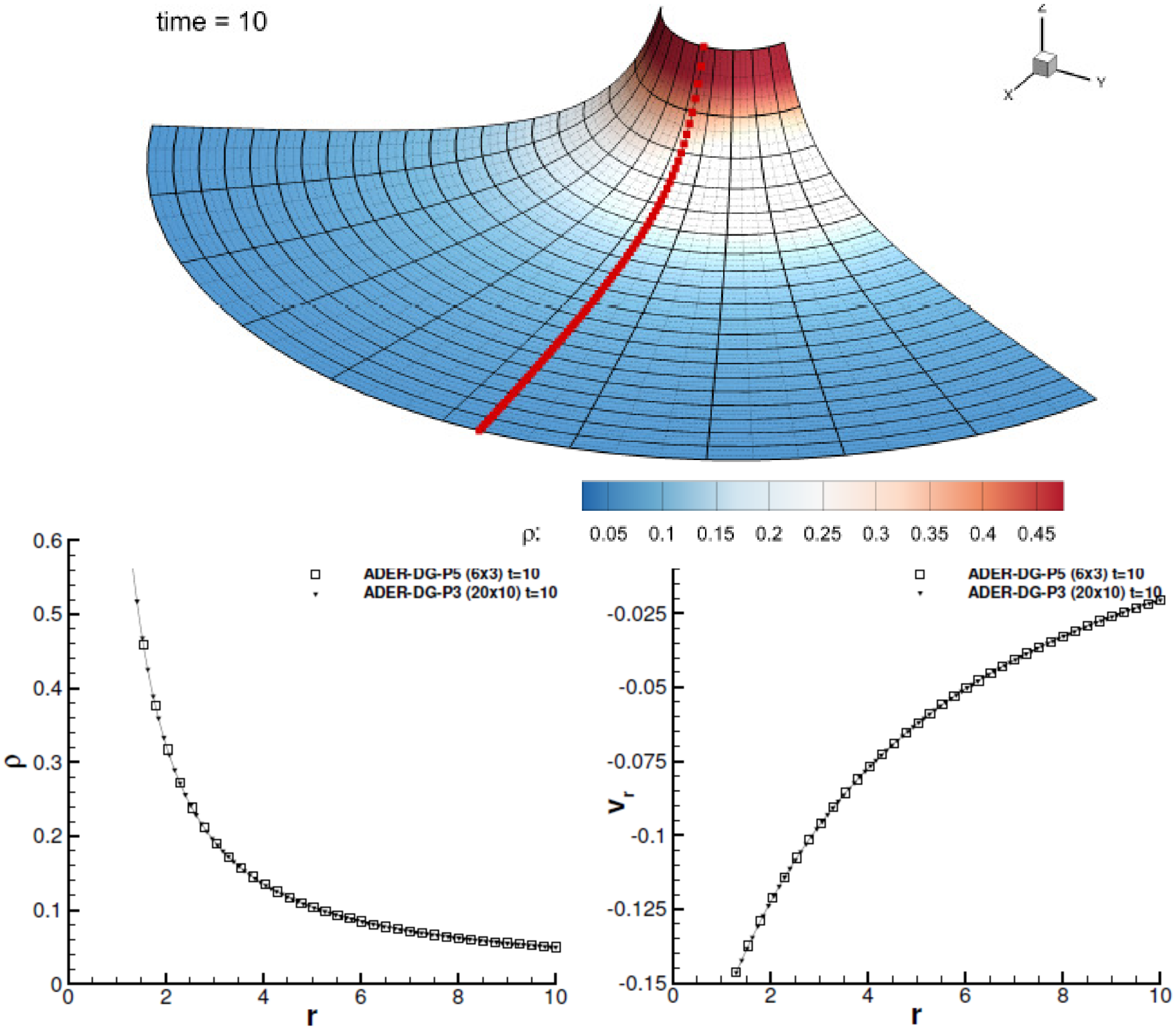

Accretion of a gas onto a black hole. GRGPR model in curved spacetime in the stiff relaxation limit. Comparison with RHD solution. Not trivial at all!

General relativistic GPR model

2D Michel accretion in KSS coordinates — ADER-DG-$\mathbb{P}_N$

			ρ		u		ρ		u		
	τ	N_x	L_1 error	L_2 error	L_1 error	L_2 error	L_1 or.	L_2 or.	L_1 or.	L_2 or.	Theor.
DG-$\mathbb{P}_2$	$\tau=10^{-5}$	10	2.68E-03	1.01E-03	6.76E-03	1.74E-03	—	—	—	—	3
		16	6.86E-04	2.67E-04	1.78E-03	4.61E-04	2.90	2.84	2.83	2.83	
		20	3.66E-04	1.44E-04	9.55E-04	2.49E-04	2.81	2.78	2.80	2.77	
		30	1.18E-04	4.61E-05	3.13E-04	8.29E-05	2.80	2.80	2.75	2.71	
DG-$\mathbb{P}_3$	$\tau=10^{-5}$	8	2.46E-04	1.52E-04	4.89E-04	1.57E-04	—	—	—	—	4
		10	9.97E-05	7.00E-05	1.70E-04	6.54E-05	4.05	3.49	4.73	3.94	
		16	1.36E-05	1.21E-05	1.81E-05	9.60E-06	4.24	3.74	4.78	4.08	
		20	5.06E-06	5.01E-06	7.23E-06	3.82E-06	4.42	3.94	4.10	4.13	
DG-$\mathbb{P}_4$	$\tau=10^{-6}$	6	1.42E-04	6.76E-05	3.79E-04	9.78E-05	—	—	—	—	5
		8	3.81E-05	2.12E-05	9.57E-05	2.65E-05	4.58	4.03	4.79	4.54	
		12	5.65E-06	3.65E-06	1.25E-05	4.02E-06	4.71	4.34	5.03	4.65	
		16	1.39E-06	1.00E-06	2.88E-06	1.05E-06	4.86	4.48	5.09	4.68	
DG-$\mathbb{P}_5$	$\tau=10^{-7}$	6	1.81E-05	1.02E-05	4.47E-05	1.24E-05	—	—	—	—	6
		8	3.69E-06	2.62E-06	8.25E-06	2.60E-06	5.53	4.74	5.87	5.44	
		10	1.05E-06	8.55E-07	2.03E-06	7.56E-07	5.65	5.02	6.29	5.54	
		12	3.56E-07	3.31E-07	6.20E-07	2.73E-07	5.92	5.21	6.49	5.59	

Stiff relaxation, comparison with ideal GRHD.

General relativistic GPR model

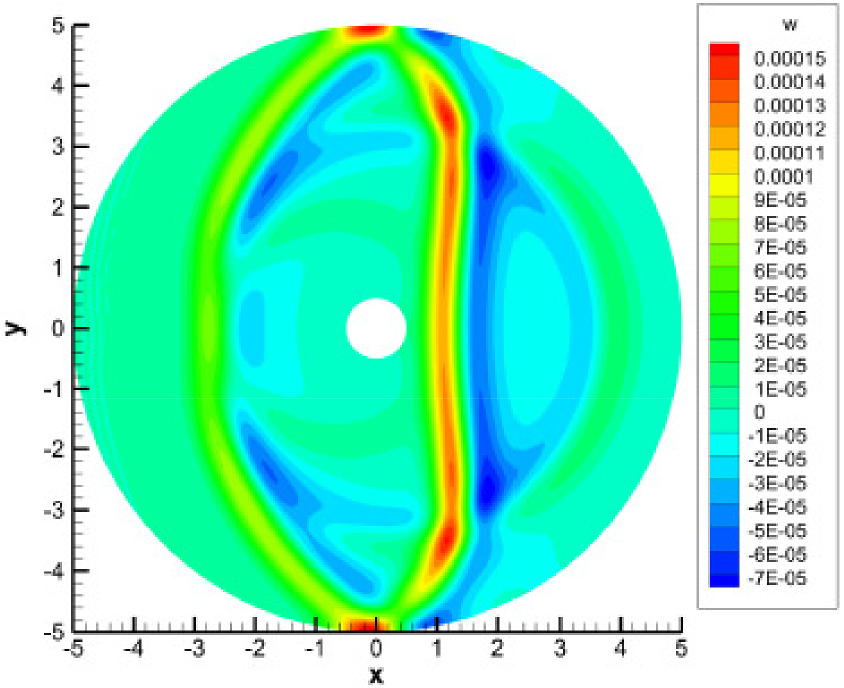

Reference solution (linear elasticity, unstructured grid in Cartesian coordinates)

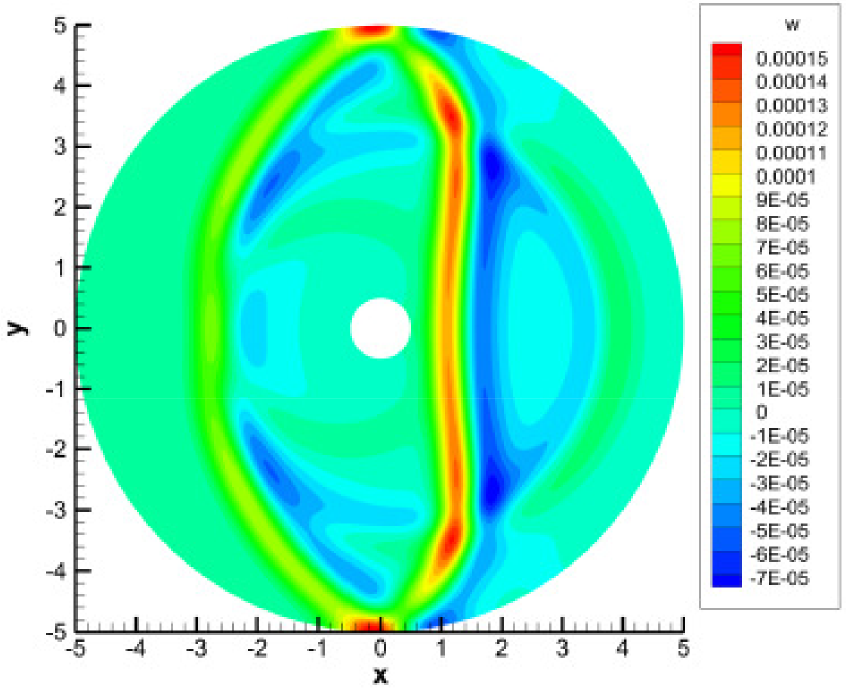

GRGPR model in cylindrical coordiantes

Seismic wave propagation in (moving) curved coordinates or on general manifolds is just a <u>special case</u> of the GRGPR model!
Here we use the Newtonian limit of the PDE to obtain a reference solution.

General relativistic GPR model

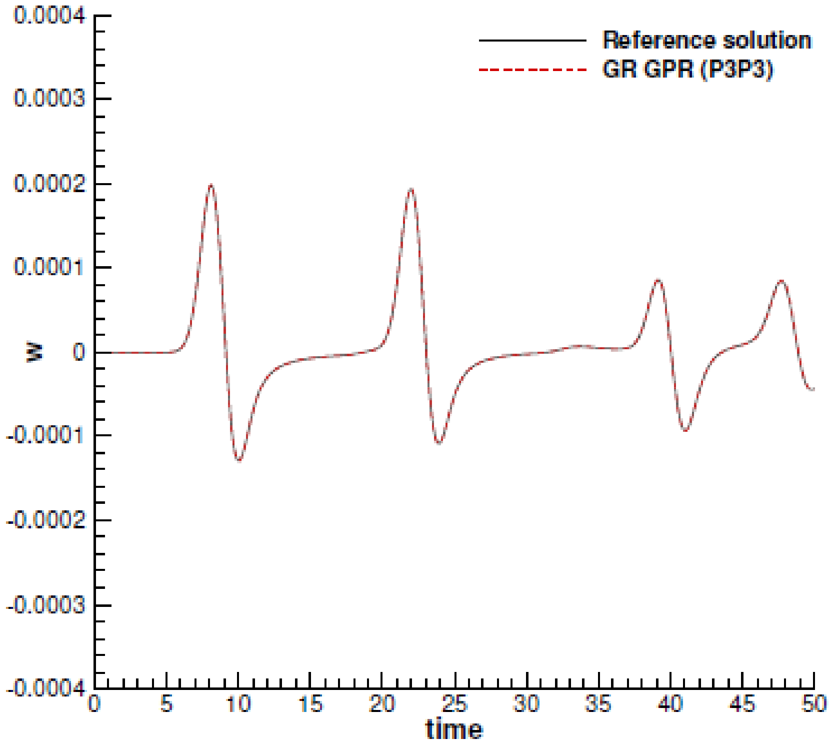

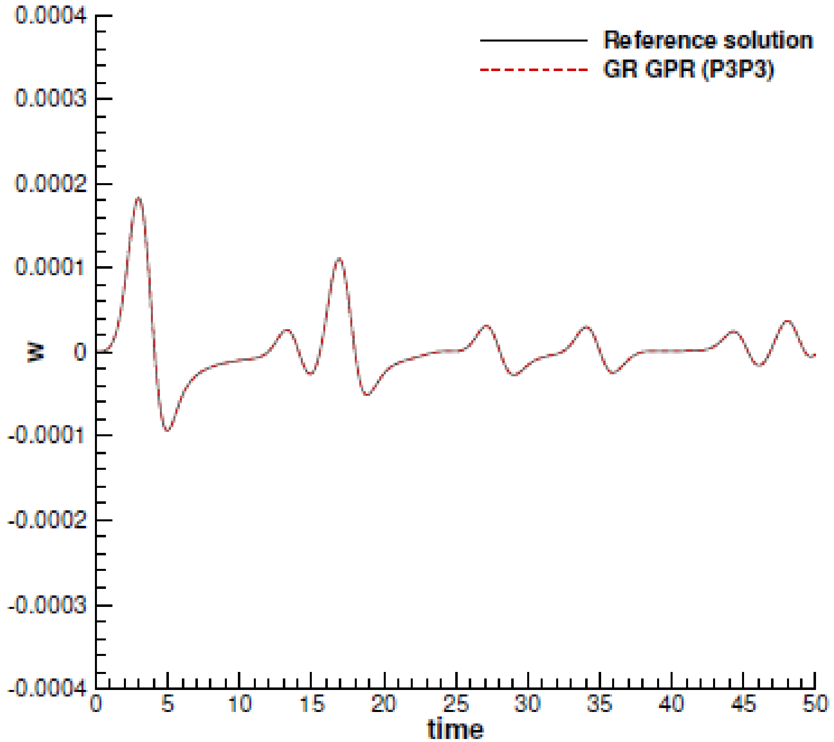

Seismic wave propagation in (moving) curved coordinates or on general manifolds is just a <u>special case</u> of the GRGPR model, thanks to general relativity! Here we use the Newtonian limit of the PDE.

Conclusions

- New high order ADER-DG schemes with a posteriori subcell FV limiter
- First order **hyperbolic** model of Newtonian continuum physics with electro-magnetic fields that covers both, fluid mechanics and solid mechanics, including viscous Newtonian fluids as well as elastic and visco-plastic solids in a single, universal formulation with **finite** wave speeds!
- Model formulation is based on the main work of **Godunov** and **Romenski** on **symmetric hyperbolic** & **thermodynamically compatible (SHTC) systems**
- Formulated for the first time by Peshkov & Romenski in 2014 and solved here numerically for the very first time.
- PDE system does not change type whether dissipative terms are present or not
- All dissipative processes have the **same structure** as the **Ohm law**
- **First** extension of the **GPR model** to the **general relativistic framework**.
- **Next natural steps: introduction of heat conduction, bulk viscosity and electromagnetic fields in the GR-GPR model.**

References

[R1] M. Dumbser, O. Zanotti, R. Loubère and S. Diot. **An a posteriori subcell limiter for discontinuous Galerkin finite element schemes**. *Journal of Computational Physics*, **278:***47-75, 2014.*

[R2] O. Zanotti, F. Fambri, M. Dumbser, A. Hidalgo. **Space–time adaptive ADER discontinuous Galerkin finite element schemes with a posteriori sub-cell finite volume limiting**. *Computers & Fluids*, **118**:204-224, 2015.

[R3] O. Zanotti, F. Fambri and M. Dumbser. **Solving the relativistic magnetohydrodynamics equations with ADER discontinuous Galerkin methods, a posteriori subcell limiting and adaptive mesh refinement**. *Monthly Notices of the Royal Astronomical Society (MNRAS)*, **452**:3010-3029, 2015.

[R4] I. Peshkov and E. Romenski. **A hyperbolic model for viscous Newtonian flows**. *Continuum Mechanics and Thermodynamics,* **28:**85–104, 2016.

[R5] M. Dumbser, I. Peshkov, E. Romenski and O. Zanotti. **High order ADER schemes for a unified first order hyperbolic formulation of continuum mechanics: viscous heat-conducting fluids and elastic solids.** *Journal of Computational Physics,* **314:**824–862, 2016

[R6] M. Dumbser, I. Peshkov, E. Romenski and O. Zanotti. **High order ADER schemes for a unified first order hyperbolic formulation of continuum mechanics coupled with electro-dynamics.** *Journal of Computational Physics,* **348:**298–342, 2017.

[R7] F. Fambri, M. Dumbser, S. Köppel, L. Rezzolla and O. Zanotti. **ADER discontinuous Galerkin schemes for general-relativistic ideal magnetohydrodynamics.** *Monthly Notices of the Royal Astronomical Society (MNRAS),* in press. https://doi.org/10.1093/mnras/sty734

[R8] M. Dumbser et al. **Conformal and covariant Z4 formulation of the Einstein equations: strongly hyperbolic first-order reduction and solution with discontinuous Galerkin schemes.** *Physical Review D* **97**, 084053 , 2018.